Agricultural and Forest Meteorology 358 (2024) 110232

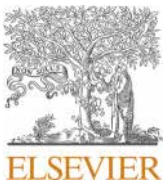

Contents lists available at ScienceDirect

Agricultural and Forest Meteorology

journal homepage: www.elsevier.com/locate/agrformet

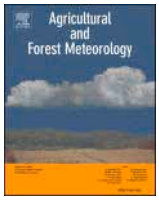

Future changes in agrometeorological extremes in the southern Mediterranean region: When and where will they affect croplands and wheatlands?

Behnam Mirgol [a,b,*], Bastien Dieppois [a], Jessica Northey [b], Jonathan Eden [a], Lionel Jarlan [c], Saïd Khabba [d,e], Michel Le Page [c], Gil Mahe [f]

[a] Centre for Agroecology, Water and Resilience (CAWR), Coventry University, Coventry, UK
[b] Centre for Peace, Trust, and Social Relations (CTPSR), Coventry University, Coventry, UK
[c] Centre for the Study of the Biosphere from Space (CESBIO), IRD, Université de Toulouse, Toulouse, France
[d] Faculty of Sciences Semlalia (LMFE), Cadi Ayyad University (UCA), Marrakech, Morocco
[e] Centre for Remote Sensing Applications (CRSA), Mohammed VI Polytechnic University (UM6P), Benguerir, Morocco
[f] HydroSciences Montpellier (HSM), CNRS, IRD, Université de Montpellier, Montpellier, France

ARTICLE INFO

Keywords:
Southern Mediterranean
Croplands
Wheatlands
Agrometeorological extremes
CMIP6

ABSTRACT

Climate change and extremes are increasingly threatening food security, especially in the Global South. Here, we examine how croplands and wheatlands of the southern Mediterranean region could be affected by projected changes in agrometeorological extremes over the 21st century. We use 17 bias-corrected climate models from the sixth phase of the Coupled Model Intercomparison Project (CMIP6) to identify potential trends and assess the time of emergence of significant changes in agrometeorological extremes under the Shared Socioeconomic Pathway (SSP3–7.0). We note that simulated historical trends in agrometeorological extremes closely match observed trends, here derived from ERA5land, over croplands. Our analysis of CMIP6 projected scenarios reveals a consistent rise in heat intensity, drought intensity, and the frequency of compound dry and hot (D5/H95) days. While a reduction in frost intensity, combined with fewer wet and cold (W95/C5) and dry and cold (D5/C5) events offer some mitigation potential, concerns about water scarcity due to heightened heat and drought stresses may overshadow these benefits. These changes in agrometeorological extremes are projected to emerge in the near- and mid-term future (by 2030 and 2050). We also note that the projected decreases in cold extremes affect smaller agricultural regions than the increases in extreme heat. We find higher likelihoods of negative agrometeorological impacts over croplands and wheatlands throughout the 21st century, which could significantly challenge crop yields and agricultural sustainability. Without proactive adaptation and mitigation strategies, food security could come increasingly under threat in a changing climate in the southern Mediterranean region.

1. Introduction

Global food production will have to be doubled by 2050 to meet the needs of the rising population and diet shifts (van Dijk et al., 2021). The frequency of extreme climate has increased in recent decades in different regions of the world (IPCC, 2022). Climate variations explain approximately a third of global crop yield variability (Ray et al., 2015; Heino et al., 2023). Additionally, the Sixth Assessment Report (AR6) of the Intergovernmental Panel on Climate Change (IPCC) suggests that the intensity and duration of climate extremes, such as drought and heatwaves, will increase and threaten long-term prospects for food security in multiple regions during the 21st century (Ostberg et al., 2018; Konduri et al., 2020; IPCC, 2022). Understanding past, present, and future trends and variability in climate, especially extremes, affecting agricultural lands, is therefore vital to enable communities to adapt and match their long-term objectives for food security (IPCC, 2022; Kumar et al., 2022). This is particularly critical in the Mediterranean region, where climate change impacts are already being felt (Raymond et al., 2019; Spagnuolo et al., 2022; Noto et al., 2023). While there has been little research on future climate change in the southern Mediterranean

* Correspondence author at: Coventry University, Coventry, UK.
E-mail address: mirgolb@uni.coventry.ac.uk (B. Mirgol).

https://doi.org/10.1016/j.agrformet.2024.110232
Received 2 July 2024; Received in revised form 4 September 2024; Accepted 8 September 2024
Available online 14 September 2024

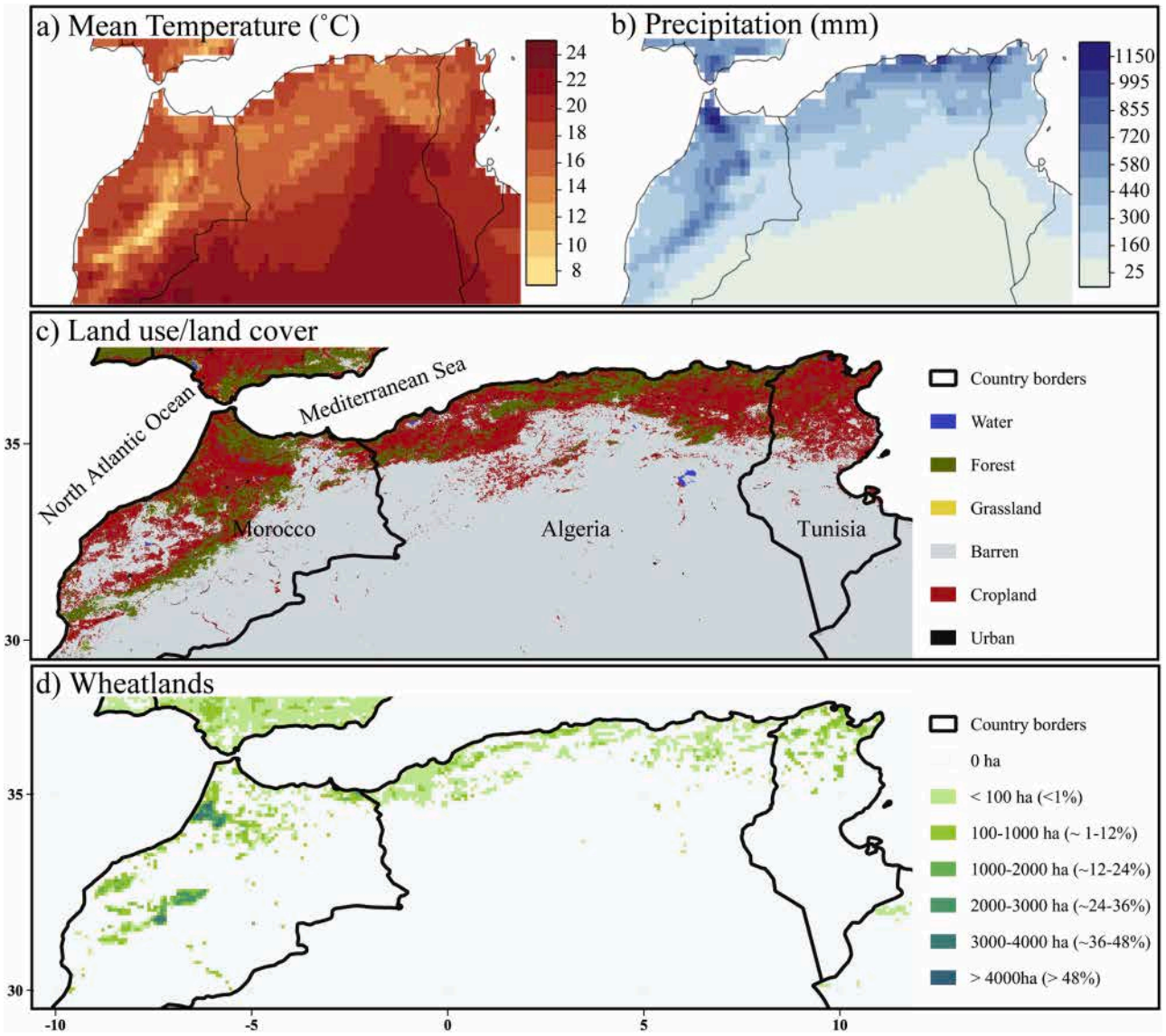

Fig. 1. Climate and landscape characteristics of the southern Mediterranean region in the historical period include (a) The annual mean temperature in ERA5land between 1995 and 2014. (b) The annual cumulative precipitation in ERA5land between 1995 and 2014. (c) The land-use/land-cover dataset from Chen et al. (2022) in the year 2015 alongside its colour-coded legend to distinguish between various land use and land cover categories. (d) The harvested wheatlands from the MIRCA2000 dataset, alongside its corresponding legend indicate the classification of harvested wheatland areas within each grid point by level and percentage.

region (North Africa and the Middle East), existing studies suggest higher rates of warming in this region compared to the rest of the world (Cramer et al., 2018; Le Page and Zribi, 2019; Gaaloul et al., 2020; Tramblay et al., 2020; Urdiales-Flores et al., 2023). Previous studies also reveal contrasting trends in future precipitation and associated extremes, underlying large uncertainties (Zittis et al., 2021; Tarín-Carrasco et al., 2024).

In a changing climate, the socioeconomic dependence of the southern Mediterranean region on the agriculture sector poses a substantial threat to sustainability (Antonelli et al., 2022; Spagnuolo et al., 2022). The effect of climate change is expected to be larger in countries relying on rain-fed agriculture, which still predominates in the southern Mediterranean (Nin-Pratt et al., 2017; Schilling et al., 2020). Although the focus of previous studies was mainly on the northern Mediterranean region, regional studies in the Mediterranean have suggested potential yield reductions in both winter and spring crops, in response to increasing frequency and severity of extreme climate weather conditions, e.g., heatwaves, droughts, coldwaves, and heavy rainfalls, during the 21st century (Saadi et al., 2015; Deryng et al., 2016; Cammarano et al., 2019; Abd-Elmabod et al., 2020; Alrteimei et al., 2022). In particular, wheat, the main staple crop in the Mediterranean region, was found to be one of the most vulnerable crops to climate change (Bouras et al., 2019; Yang et al., 2020; Zampieri et al., 2020). Existing studies, discussing the impact of climate change on crop production, however, rely on climate models from the third and fifth phases of the Coupled Model Intercomparison Project (CMIP3/5), which were used in the fourth and fifth IPCC Assessment Reports (AR4 and AR5) (Schilling et al., 2012; Chourghal et al., 2016; Bouabdelli et al., 2022; Kourat et al., 2022), and use emission scenarios that are not up to date, potentially incomplete or unrealistic (O'Neill et al., 2020). In addition, previous regional agrometeorological impact studies do not systematically employ bias correction techniques to increase the spatial resolution of the climate model outputs and remove any systematic biases (Maraun and Widmann, 2018). It is therefore crucially important to re-evaluate future changes using robust state-of-the-art climate change models and scenarios, such as those presented in the sixth phase of CMIP (CMIP6).

Estimating the time of emergence (ToE) for significant changes in extreme weather conditions over the 21st century is essential for better

Table 1
Information on the bias-corrected CMIP6 models used in this study.

Name of GCM	Model centre/country	Reference
ACCESS-CM2	Commonwealth Scientific and Industrial Research Organization, Australia	Bi et al. (2020)
BCC—CSM2-MR	Beijing Climate Centre and China Meteorological Administration, China	Wu et al. (2020)
CanESM5	Canadian Centre for Climate Modelling and Analysis, Canada	Swart et al. (2019)
CMCC-ESM2	The Euro-Mediterranean Centre on Climate Change, Italy	Lovato et al. (2022)
CNRM-ESM2–1	Centre National de Recherches Météorologiques–Centre Européen de Recherche et de Formation Avancée en Calcul Scientifique, France	Séférian et al. (2019)
EC-Earth3-Veg-LR	EC-EARTH consortium, Sweden	Döscher et al. (2022)
FGOALS-g3	LASG, Institute of Atmospheric Physics, Chinese Academy of Sciences, China	Li et al. (2020)
GFDL-ESM4	NOAA Geophysical Fluid Dynamics Laboratory, USA	Horowitz et al. (2020)
GISS-E2–1-G	NASA/GISS (Goddard Institute for Space Studies), USA	Kelley et al. (2020)
INM-CM5–0	Institute for Numerical Mathematics, Russian Academy of Science, Moscow, Russia	Volodin et al. (2019)
IPSL-CM6A-LR	L'Institut Pierre–Simon Laplace, France	Boucher et al. (2020)
KACE-1–0-G	National Institute of Meteorological Sciences/Korea Meteorological Administration, Korea	Lee et al. (2020)
MIROC6	Japan Agency for Marine-Earth Science and Technology, Atmosphere and Ocean Research Institute, Japan	Takemura and Toshihiko (2019)
MPI-ESM1–2-LR	Max Planck Institute, Germany	Wieners et al. (2019)
MRI-ESM2–0	Meteorological Research Institute (MRI), Japan	Yukimoto et al. (2019)
NorESM2-LM	Climate Modelling Consortium, Norway	Seland et al. (2019)
UKESM1–0-LL	Met Office Hadley Centre, UK	Sellar et al. (2019)

Table 2
Summary of analysed agrometeorological hazards over croplands.

Indicator	Description and Impacts
Maximum heat intensity	**Definition:** Annual maximum deviation of daily maximum temperature from the 95th percentile. **Potential Impact:** Heat stress can disrupt plant growth cycles, reduce pollination rates, and scorch leaves and fruits, leading to significant yield losses (Bernacchi et al., 2023; Hatfield and Prueger, 2015).
Maximum drought intensity	**Definition:** Annual minimum seasonal Standardized Precipitation Evapotranspiration Index (SPEI) value. The SPEI integrates monthly precipitation and potential evapotranspiration, standardized using the generalised extreme value (GEV) distribution for comparisons across locations and periods (Vicente-Serrano et al., 2010). A rectangular kernel function is applied to give equal weight to all the data integrated over a three-month period. The reference period used for parameter fitting is set to 1955–2100. The potential evapotranspiration is computed using the Hargreaves equation modified by Droogers and Allen (2002). **Potential Impact:** Droughts can severely limit water availability for plants, hindering growth, reducing photosynthesis, and ultimately leading to crop failure (Mirgol et al., 2020; Seleiman et al., 2021; Nazari et al., 2021)
Maximum frost intensity	**Definition:** Annual maximum deviation of daily minimum temperature (only negative values) from 0 °C. **Potential Impact:** Frost events can have a stage-specific damaging impact on plant growth, reducing yields or causing entire crop failures (Jagannathan, 2019; Parker et al., 2021).
Maximum extreme precipitation intensity	**Definition:** Annual maximum deviation of daily precipitation from the 95th percentile. **Potential Impact:** Heavy precipitation can cause waterlogging, soil erosion, and nutrient leaching, all of which have a detrimental influence on crop health and yield (Kaur et al., 2019).
Number of dry and hot days (D5/H95)	**Definition:** Annual number of days when daily precipitation falls below the 5th percentile and daily mean temperature exceeds the 95th percentile, simultaneously. **Potential Impact:** The increased co-occurrence of drought and heat stresses exacerbates crop growth conditions, leading to further reductions in crop yields (Guion et al., 2021).
Number of wet and hot days (W95/H95)	**Definition:** Annual number of days when daily precipitation and mean temperature exceed the 95th percentile, simultaneously. **Potential Impact:** While some crops might benefit from the increased water availability, very hot and wet conditions can promote the spread of plant diseases and hinder pollination, potentially reducing yields (Velásquez et al., 2018; Singh et al., 2023).
Number of wet and cold days (W95/C5)	**Definition:** Annual number of days when daily precipitation exceeds the 95th percentile and daily mean temperature falls below the 5th percentile, simultaneously. **Potential Impact:** The increased co-occurrence of frost days and heavy precipitation events can inflict more severe damage on crop production than experiencing either event alone (Mirgol et al., 2023).
Number of dry and cold days (D5/C5)	**Definition:** Annual number of days when daily precipitation and mean temperature fall below the 5th percentile, simultaneously. **Potential Impact:** Extended cold and dry periods can delay planting, shorten growing seasons, and potentially damage crops depending on their specific cold tolerance (Mirgol et al., 2023).

decision-making and smarter planning for climate change adaptation, particularly in the under-researched southern Mediterranean region. Previous studies underscore the importance of identifying the ToE for new climate extremes that significantly differ from past and present conditions (Hawkins and Sutton, 2012; Lehner et al., 2017; Gaetani et al., 2020). Such analyses are crucial for developing robust risk assessments, optimising resource allocations, and designing appropriate policies across the southern Mediterranean region. This paper specifically assesses the ToE regarding significant positive and negative changes in agrometeorological extremes that affect croplands and wheatlands in this region. Moreover, compound extremes often exacerbate the impacts and result in substantial reductions in crop yield, making the coexistence of climate extremes more damaging than individual events. Earlier studies have shown that simultaneous dry and hot conditions have triggered poor harvests and up to 30 % yield reductions globally since the early 2000s (Ribeiro et al., 2020; Zscheischler et al., 2020; Lesk et al., 2022; Velpuri et al., 2023). Similarly, an increased occurrence of such compound extremes has posed significant threats to Mediterranean crop production over the last four decades (Vogel et al., 2021). Yet, the potential implications of future changes in compound extremes (e.g., dry and hot, dry and cold, wet and hot, and wet and cold) on crop production remain largely unexplored in the southern Mediterranean context. This research gap highlights the necessity for comprehensive analyses that consider both the timing and the compounded nature of extreme weather events in order to sustain agricultural productivity in this vulnerable region.

In this paper, we aim to identify potential trends in agrometeorological extremes, including compound events, over the southern Mediterranean region during the 21st century using bias-corrected climate change scenarios from CMIP6 models. Specifically, we assess where and when significant changes in agrometeorological extremes are more likely to affect croplands and wheatlands, and potentially combine their impacts during the 21st century. The structure of our paper is as

Table 3
Summary of analysed agrometeorological hazards over wheatlands and their potential impacts within the reproductive phase of winter wheat.

Indicator	Description and Impacts
Maximum heat shock	**Definition:** maximum deviation of daily maximum temperature from 30 °C during the reproductive phase of winter wheat.**Potential Impact:** • Heat stress reduces grain number (sterility and abortion of grains) during flowering to early grain filling (Barlow et al., 2015). • It shortens the duration of grain filling affecting final grain weight (Dias and Lidon, 2009). • Post-heading heat stress can significantly explain the grain yield variability (Liu et al., 2014).
Maximum drought intensity	**Definition:** minimum seasonal SPEI value during the reproductive phase of winter wheat.**Potential Impact:** • The flowering and grain-filling stages are the most sensitive periods for winter wheat, when even a mild drought can significantly decline yield (Yu et al., 2018; Mirgol et al., 2020). • Droughts between the Booting and Heading stages reduce the yield (Zhang et al., 2021).
Maximum frost intensity	**Definition:** maximum deviation of daily minimum temperature from −4 °C during the reproductive phase of winter wheat.**Potential Impact:** • Wheat tolerates frosts during its vegetative growth stages but becomes increasingly susceptible during flowering, particularly in early spring, and a short period of freezing temperatures during the reproductive phase can severely damage it (Cheong et al., 2019; Frederiks et al., 2015). • Frost can cause significant reductions in yield due to the plant's heightened sensitivity and diminished cold acclimation in the reproductive phase (Hassan et al., 2021). • Frost's most significant impacts are sterility and grain abortion around flowering (Barlow et al., 2015).
Nb DH days	**Definition:** number of days within the winter wheat reproductive phase when both daily precipitation is below one millimetre and daily mean temperature surpasses 30 °C. **Potential Impact:** • Concurrent dry and hot events exacerbate the negative impacts on wheat yields, particularly during the reproductive phase (Mahrookashani et al., 2017; Zampieri et al., 2017; He et al., 2024).
Nb DC days	**Definition:** number of days within the winter wheat reproductive phase when both daily precipitation is below one millimetre and daily mean temperature falls below −4 °C.**Potential Impact:** • The combination of extreme dry and cold events has more devastating impacts on wheat yield, particularly during its reproductive phase (Mirgol et al., 2024).

follows. Section 2 describes the study area, data, and methods. In Section 3, we first analyse potential trends in projected changes of eight agrometeorological extreme indicators, before assessing their ToE and capacity to combine their impacts over croplands and wheatlands. Finally, in Section 4, we conclude and engage in a discussion exploring the broader implications of our findings.

2. Study area, data, and methods

2.1. Study area

This study focuses on Morocco, Algeria, and Tunisia, which account for the majority of the southern Mediterranean croplands (Benabdelkader et al., 2021). This region is known for its climatic diversity, ranging from a temperate climate in the north to arid regions in the south, marked by hot and dry summers and temperate and wet winters (Abd-Elmabod et al., 2017). The annual mean temperature of the region exhibits a considerable range, varying from 8 °C in mountainous northern regions to 24 °C in the Sahara Desert (Fig. 1a). Presently, these temperatures are approximately 1.5 °C higher than pre-industrial era, surpassing the global warming average of +1.1 °C (Zribi et al., 2020). Furthermore, the region displays diverse annual mean precipitation levels, ranging from 25 mm.year^{-1} in the south to over 1100 mm.year^{-1} in the Atlas Mountain in Morocco (Fig. 1b).

Various land use and land cover categories define the landscape of this region, but croplands stand out as a pivotal feature, particularly in the northern and coastal areas (Fig. 1c). Additionally, agriculture in the Sahara has experienced remarkable growth over the past few decades, notably in Algeria, as a result of proactive policies and the existence of great potential in groundwater resources (Bouchemal, 2021). These croplands not only contribute significantly to the regional economy but also offer the opportunity to export an estimated USD 13.8 billion worth of agricultural products, particularly to Europe (Statista Research Department, 2024a, b, c). Moreover, wheat, one of the three major cereal crops providing daily calories and proteins worldwide, holds prominence in the agricultural landscape of this region concentrated in the northern areas (Awika, 2011; Giraldo et al., 2019; Fig. 1d). Wheatlands ensure the food security of the region and play a vital role in the economies of Morocco, Algeria, and Tunisia by producing around 11.2 million metric tonnes in the marketing year 2021–2022 (USDA, 2024).

2.2. Climate data

To reduce the uncertainties inherent in climate modelling and enhance the reliability of our analyses, we utilise the latest version of the NASA Earth Exchange Global Daily Downscaled Projections (NEX-GDDP-CMIP6) described by Thrasher et al. (2022). These projections incorporate downscaled historical and future data from 1955 to 2100, derived from CMIP6 outputs. The downscaled datasets were generated utilising a daily version of the monthly bias correction/spatial disaggregation technique, as outlined by Wood et al. (2004) and Thrasher et al. (2012), resulting in a horizontal resolution of 0.25° Specifically, we used 17 downscaled and bias-corrected CMIP6 models (Table 1). According to the findings of Masson and Knutti (2011) on the significant similarities and dependencies among climate models from the same institutions, we selected only one climate model from each institution. Similarly, based on O'Neill et al. (2020) recommendations, we restricted our analysis to the most plausible emission and forcing scenarios, i.e., the Shared Socioeconomic Pathway 3–7.0 (SSP370) scenario. The SSP370 scenario represents a medium-high socioeconomic development path with radiation forcing peaking at 7.0 W/m^2 by the end of the century (O'Neill et al., 2020; Tang et al., 2022).

Furthermore, we assess how simulated historical trends and variations in agrometeorological extremes compare to observed trends and variations, using the ERA5land reanalysis dataset (https://cds.climate.copernicus.eu/cdsapp#!/dataset/reanalysis-era5-land?tab=overview). ERA5land is the fifth-generation atmospheric reanalysis from the European Centre for Medium-Range Weather Forecasts (ECMWF), offering a wide set of meteorological variables at a high spatial resolution of 0.1° × 0.1° (Muñoz-Sabater et al., 2021). Reanalysis datasets combine historical observations from across the world with advanced atmospheric models to create a consistent and complete picture of Earth's climate system using the laws of physics. In this study, we extracted daily maximum temperature, minimum temperature, mean temperature, and total precipitation from 1955 to 2014.

2.3. Land-use/land-cover dataset

To assess the potential vulnerability of croplands to future climatic changes, we employ a global land use and land cover (LULC) dataset provided by Chen et al. (2022) (http://www.geosimulation.cn/Global-SSP-RCP-LUCC-Product.html). This dataset provides a 1-km global LULC dataset with seven distinct LULC categories, facilitating our

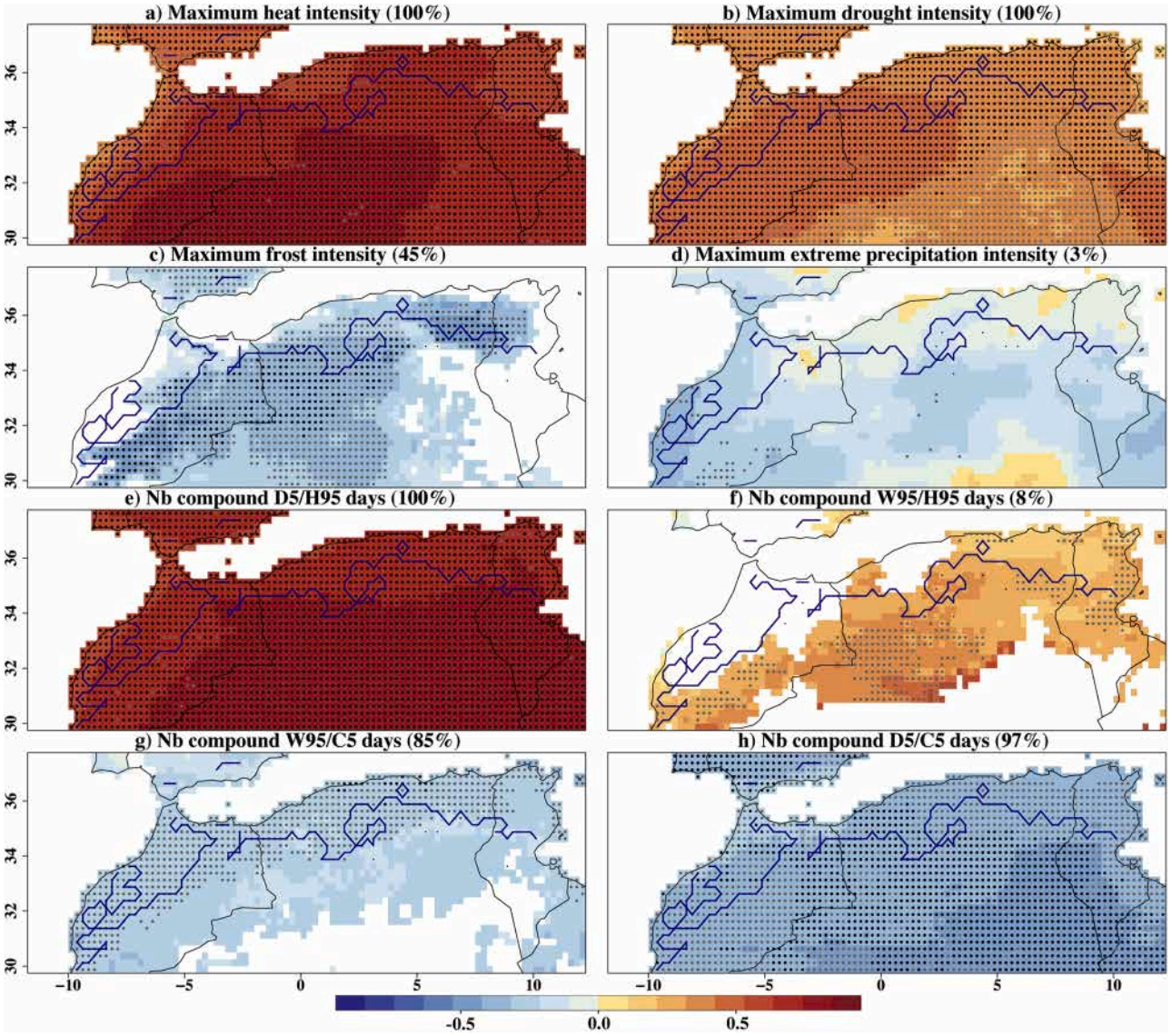

Fig. 2. Spatial distribution of CMIP6 multi-model mean projected trends (2015–2100) in agrometeorological extremes over the southern Mediterranean region under the SSP370 scenario. Each subplot represents the multi-model mean trend of a specific agrometeorological indicator, including maximum intensities in (a) heat, (b) drought, (c) frost, and (d) extreme precipitation, alongside the number of extreme compound events in (e) D5/H95, (f) W95/H95, (g) W95/C5, and (h) D5/C5. Kendall's Tau (blue to red shading) is used to measure the direction and rate of changes in different indicators. Black and grey dots show grid points where at least 90 % and 50 % of the models agree on the sign of significant changes, respectively. Dark blue contour lines indicate the cropland extent in the LULC dataset in 2015. Numbers in the parenthesis indicate the estimated percentages of these croplands that would be influenced by each significant climate extreme.

understanding of cropland dynamics over the 21st century. It integrates top-down land demand constraints from CMIP6 data and the bottom-up spatial simulation using cellular automata (CA) and an Artificial Neural Network (ANN), ensuring the accuracy of the land trajectories under different SSP-RCP scenarios. The CA model is executed regionally to capture spatial heterogeneity. Here, we focus on croplands, including both rainfed and irrigated areas, under the SSP370 scenario over the southern Mediterranean region. Given the higher resolution of the LULC dataset compared to CMIP6 models, we define areas as croplands when they cover at least 100 hectares of a climate model's pixel.

Additionally, we employ the Monthly Irrigated and Rainfed Crop Areas around the year 2000 dataset (MIRCA2000; https://www.uni-frankfurt.de/45218031/Data_download_center_for_MIRCA2000), which provides information on both irrigated and rainfed crop areas for 26 crop classes at a resolution of 5 arc-minutes, equivalent to approximately 0.08° (Portmann et al., 2010). This dataset provided us with the location and proportion of the harvested wheatland areas in the historical period. This parallel assessment extends our focus to wheatlands, as one of the most strategic crops in the southern Mediterranean region, enabling a more in-depth exploration of the potential influences of climatic extreme events on both croplands and wheatlands. Due to the coarser resolution of CMIP6 models, we establish a minimum 100-hectare wheatland cover threshold within each climate model's pixel to identify wheatland areas over the region.

2.3. Methodology

2.3.1. Analysing agrometeorological extremes and their impacts on crop production

In this study, we first focus on eight extreme agrometeorological indicators, each associated with specific impacts on croplands. These indicators encompass maximum intensities in individual extreme events and the frequency of compound extreme events across the calendar year, both recognized as vital factors influencing crop growth and

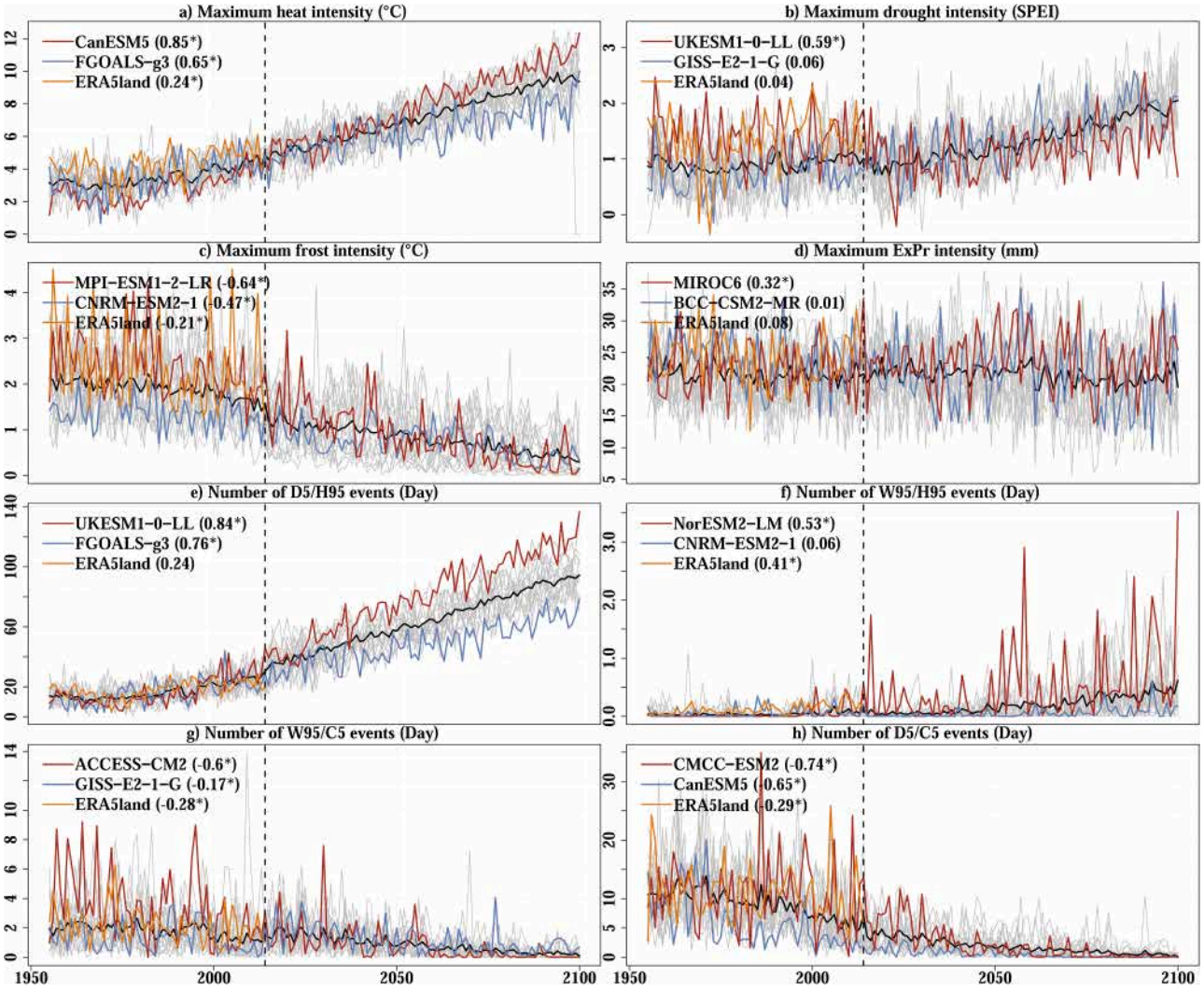

Fig. 3. Temporal evolution of observed and simulated agrometeorological extremes between 1955 and 2100 under the SSP370 scenario. Each subplot represents a specific agrometeorological indicator and its trends in ERA5land, 17 bias-corrected CMIP6 models and their multi-model ensemble mean, including maximum intensities in (a) heat, (b) drought, (c) frost, and (d) extreme precipitation, alongside the number of extreme compound events in (e) D5/H95, (f) W95/H95, (g) W95/C5, and (h) D5/C5. The black lines depict multi-model ensemble mean values. On each panel, the red and blue lines indicate the corresponding most and least pronounced trends across all climate models, respectively. The orange line shows the trends of each indicator in the ERA5land dataset. Dashed lines divide the periods into two historical and future scenarios. Kendall's Tau is used to measure the magnitude of the trends, which are shown in parentheses, with asterisks indicating significant trends at a 95 % confidence level.

development. Table 2 outlines the details of these indicators.

We also analyse future changes in agrometeorological extremes during the most sensitive phenological stages of winter wheat growth to climatic changes. According to previous studies (Barnabás et al., 2008; Yang et al., 2020), the reproductive phase, which includes booting, heading, flowering, milk development, and grain filling, is the most sensitive stage to climatic changes (Ahmad et al., 2021; Epule et al., 2022; Hu et al., 2022). In the southern Mediterranean region, the reproductive phase of winter wheat occurs between February and June, varying by cultivation zone (Latiri et al., 2010; Epule et al., 2022). During the reproductive phase, wheat is developing its flowers and seeds, and exposure to climatic stresses, such as severe cold/hot temperatures and drought, can damage the pollen grain, reduce the grain number/ear, and reduce the filling rate, which leads to significant yield reductions (Yu et al., 2018; Suresh and Munjal, 2020). Here, we, therefore, evaluate potential future changes in maximum heat shocks, drought intensity, frost intensity, and the combinations of drought with heatwave and frost events during the reproductive stage of winter wheat growth, incorporating insights from overlapping various existing phenological calendars over the southern Mediterranean region. Table 3 provides more details about the selected extreme event indicators and the potential impacts of these extreme events on the reproductive phase of winter wheat growth and development.

2.3.2. *Trend analysis in agrometeorological extremes*

To analyse both past (1955–2014) and future (2015–2100) trends in various agrometeorological extremes, we apply the Mann-Kendall (MK) statistical test (Mann, 1945; Kendall, 1948). The MK test, known for its wide use in hydrology, climate research, and environmental science (Yue et al., 2002; Hu et al., 2020), is a non-parametric method that relies on ranking data instead of their actual distribution (Wang et al., 2020). To address the possibility of serial correlation within our data, we used a modified version of the MK test introduced by Hamed and Ramachandra Rao (1998). This modified approach estimates effective degrees of freedom and adjusts p-values based on autoregressive coefficients. Meanwhile, the MK Tau value is used to quantitatively evaluate the direction and magnitude of trends across all projected bias-corrected CMIP6 models.

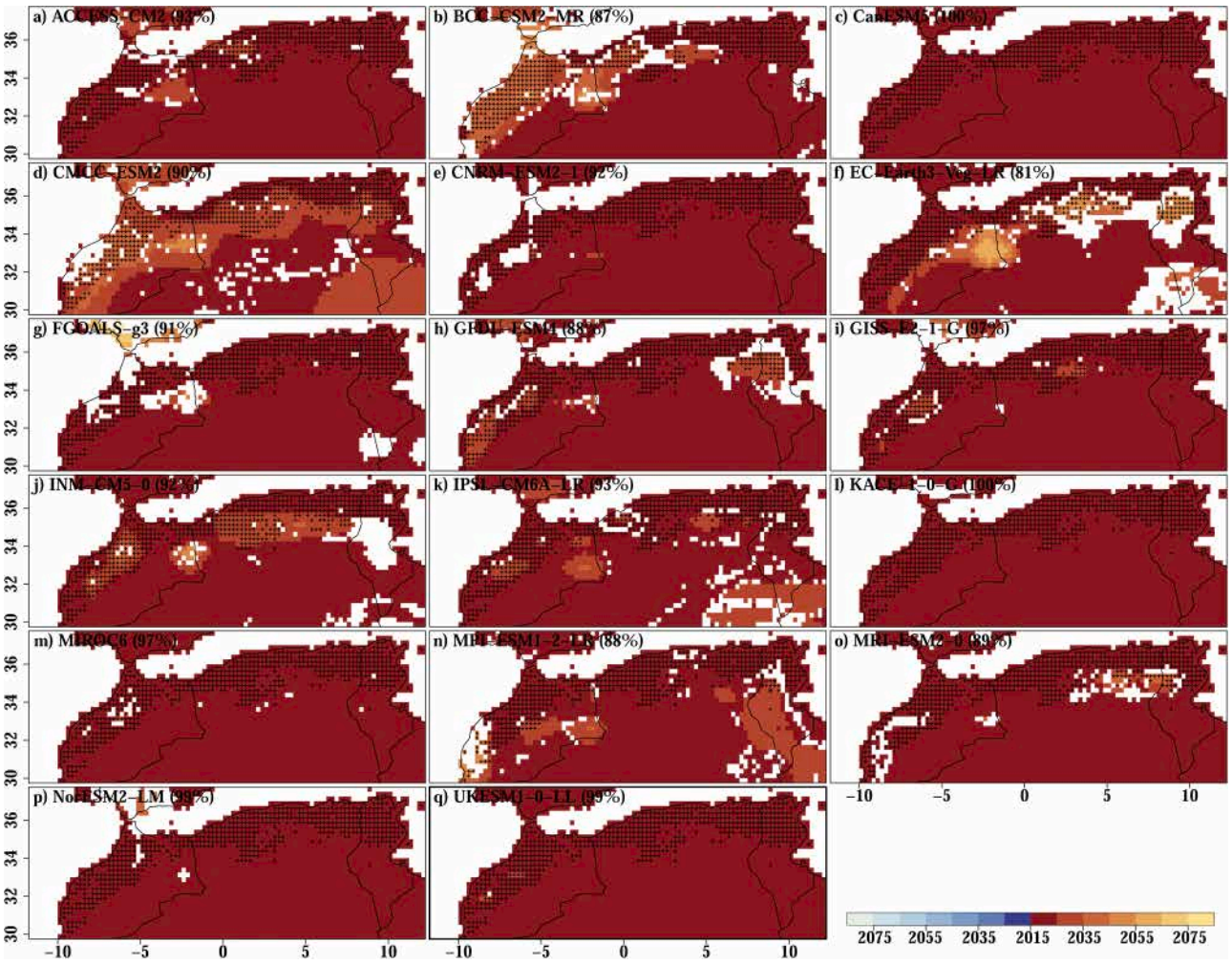

Fig. 4. Spatial and temporal distributions of ToE for the maximum heat intensity in 17 bias-corrected CMIP6 models under the SSP370 scenario over the southern Mediterranean region. For all models (**a**-q), red (blue) shades show ToE for significant increases (decreases) in Maximum heat intensity compared to the reference period (1995–2014). Plus (+) signs show the locations of croplands where the median of projected agrometeorological indicators significantly differs from the median of the historical period based on the Wilcoxon test at a 95 % confidence level. Numbers in parentheses indicate the percentage (%) of croplands that could be impacted by significant increases in maximum heat intensity by the end of the 21st century.

We summarize the results of the trend analysis using multi-model ensemble means for each grid point across the southern Mediterranean region. Additionally, we quantify the percentage of CMIP6 models showing a significant increase or decrease in agrometeorological indicators at $p \leq 0.05$. We also estimate the proportion of croplands affected by significant trends, incorporating the LULC dataset in 2015. To assess the regional trends in CMIP6 models over the years and compare them with those observed during the historical period, we calculated the regional average of each indicator for both the CMIP6 models and ERA5land.

2.3.3. *ToE of significant changes in agrometeorological extremes*

The ToE is here defined as the specific time (year) in the 21st century when agrometeorological extremes are significantly different from past and present conditions in terms of intensity and/or frequency. To calculate the ToE in the agrometeorological hazard indicators, for each model and each grid point, we first calculate the median of the projected agrometeorological indicators using a 20-year running window, sliding across the period from 2015 to 2100. Then, we compared all the future 20-year running medians to the median simulated over a historical baseline (1995–2014). To assess the significance of future changes, we employ the Wilcoxon test, a non-parametric statistical test well-suited for comparing paired samples when the data distribution is non-normal (Wilcoxon, 1945). Finally, we define the ToE as the start of the 20-year period for which the median is significantly different from the median of the historical period, as determined by the Wilcoxon test at a 95 % confidence level. In addition, regardless of the change being significantly positive or negative, the ToE must be irreversible, with the new climate condition enduring until the century's close. Moreover, given that ToE detection can be affected by distribution sizes, we also conducted ToE calculations using 15-year and 25-year time windows. The results were quite similar to those obtained with the selected 20-year window (not shown).

Furthermore, to provide a synthesis of potential cumulated negative and positive agrometeorological impacts, we estimate the fraction of croplands and wheatlands that could be affected by the emergence of one or multiple significant changes in agrometeorological extremes of the multi-model mean of bias-corrected CMIP6 models under the SSP370 scenario in the near-term (by 2030), mid-term (by 2050), and long-term (by 2100) future. We consider a significant change to have a negative impact on crops when it could potentially decrease crop productivity, and vice versa for positive impacts (cf. Tables 2-3).

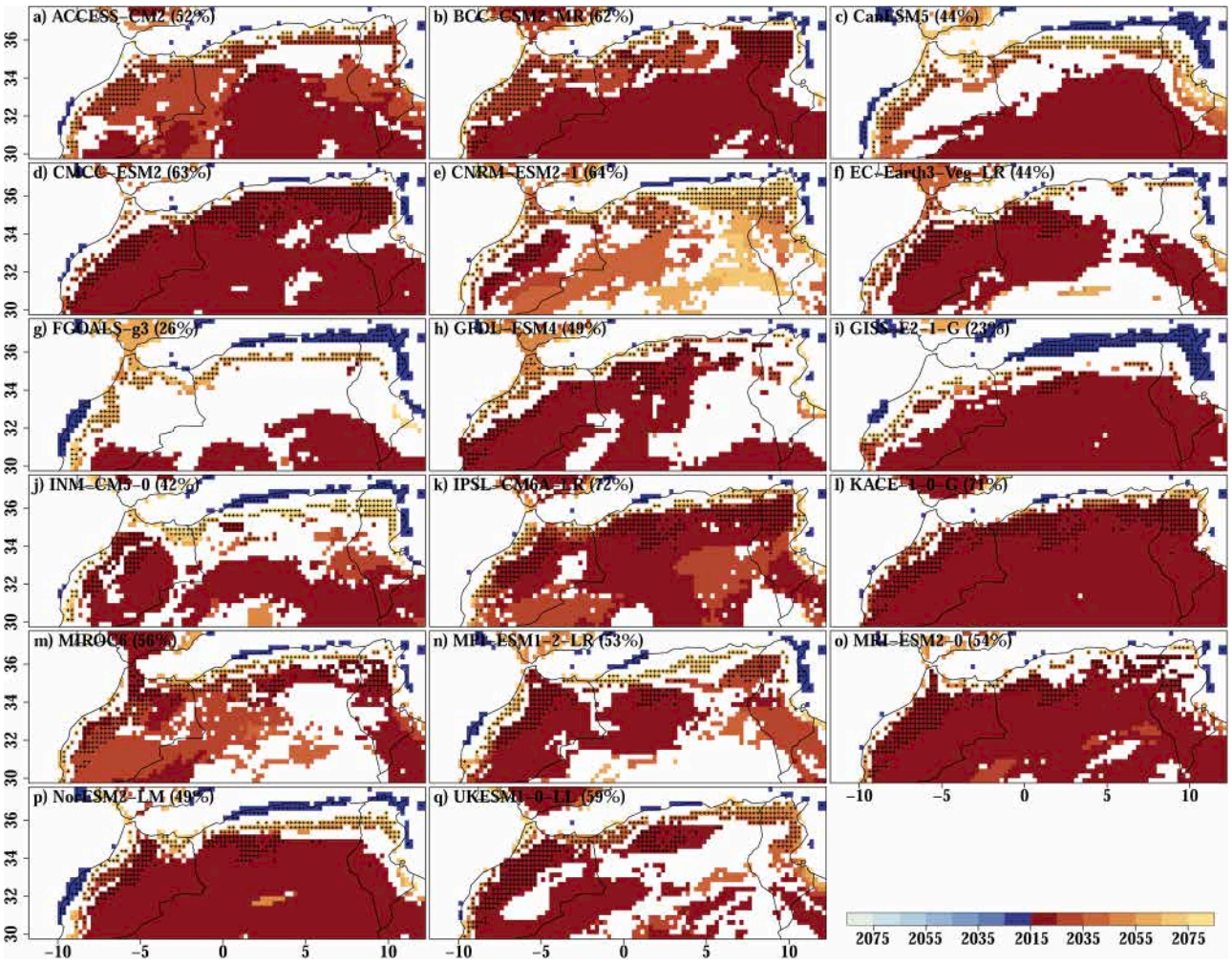

Fig. 5. Spatial and temporal distributions of ToE for maximum drought intensity in 17 bias-corrected CMIP6 models under the SSP370 scenario over the southern Mediterranean region. For all models (**a**-q), red (blue) shades show ToE for significant increases (decreases) in maximum drought intensity compared to the reference period (1995–2014). Plus (+) signs show the locations of croplands where the median of projected agrometeorological indicators significantly differs from the median of the historical period based on the Wilcoxon test at a 95 % confidence level. Numbers in parentheses indicate the percentage (%) of croplands that could be impacted by significant changes in maximum drought intensity by the end of the 21st century.

3. Results

3.1. Multi-model agreement in climatic trends over the southern Mediterranean croplands

We examine the potential occurrence of significant trends in different agrometeorological extreme indicators over the southern Mediterranean using 17 bias-corrected CMIP6 models. For simplicity, Fig. 2 displays the multi-model mean monotonic trend magnitude (Tau) and the multi-model agreement in simulating significant trends across the 17 CMIP6 models. Using the LULC data shown in Fig. 1c, we also estimate the proportion of croplands affected by significant decreasing and increasing trends in these indicators between 2015 and 2100.

Significant increasing trends in maximum heat intensity, maximum drought intensity, and the number of D5/H95 events are consistently found across climate models (>90 % model agreement) and 90 % of grid points in the southern Mediterranean region. In addition, we note that these trends could affect 100 % of croplands over the region in the 21st century (Figs. 2a, b, e). Similarly, in most climate models (>50 % model agreement), the number of W95/H95 events shows increasing trends, affecting 8 % of the croplands in north-eastern Algeria and northern Tunisia (Fig. 2f).

We also found significant decreasing trends in maximum frost intensity, and the number of W95/C5 and D5/C5 events in many climate models, with over 50 % of models agreeing. Specifically, these decreasing trends are evident in 43 %, 33 %, and 98 % of the grid points, respectively (Figs. c, g, h). Decreasing maximum frost intensity could affect 45 % of croplands in the southern Mediterranean region (Fig. 2c). Meanwhile, decreasing the number of W95/C5 and D5/C5 events will likely affect 85 % and 97 % of croplands, respectively (Figs. 2g, h). However, we do not find robust and significant trends in the maximum precipitation intensity over the southern Mediterranean region (Fig. 2d). Significant trends in maximum precipitation intensity are found in over 4 % of the region, and only 3 % of croplands, across half of the climate models analysed (Fig. 2d).

In summary, in bias-corrected CMIP6 models, southern Mediterranean croplands are likely to be increasingly exposed to extreme heat and drought during the 21st century, which could pose a significant threat to crops, reducing the yields (del Pozo et al., 2019; Heino et al., 2023). Meanwhile, the models suggest decreasing cropland exposure to cold extremes over the 21st century, which could positively impact crop yield (Abi Saab et al., 2019).

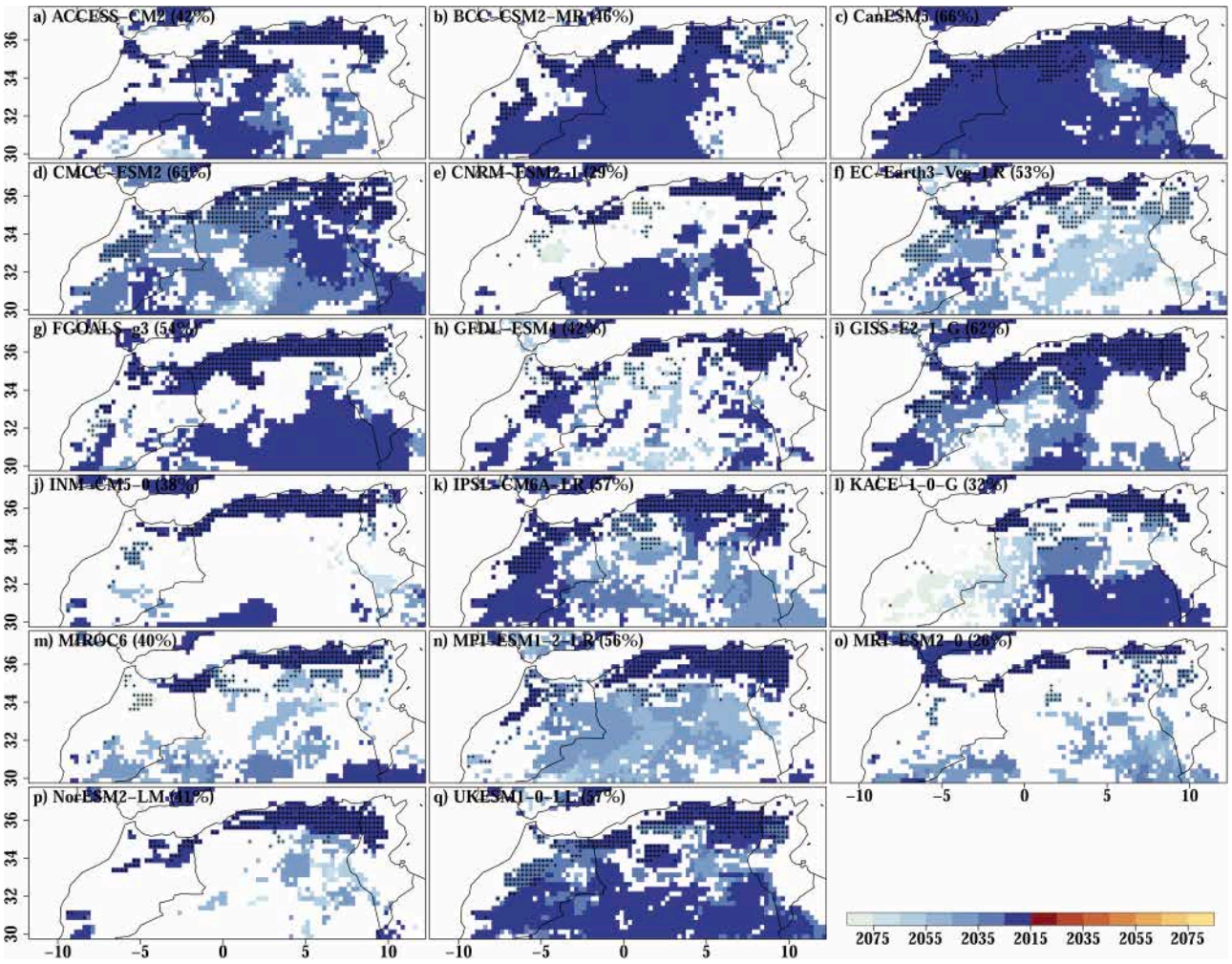

Fig. 6. Spatial and temporal distributions of ToE for maximum frost intensity in 17 bias-corrected GCMs under the SSP370 scenario over the southern Mediterranean region. For all models (**a**-q), red (blue) shades show ToE for significant increases (decreases) in maximum frost intensity compared to the reference period (1995–2014). Plus (+) signs show the locations of croplands where the median of projected agrometeorological indicators significantly differs from the median of the historical period based on the Wilcoxon test at a 95 % confidence level. Numbers in parentheses indicate the percentage (%) of croplands that could be impacted by significant decreases in maximum frost intensity by the end of the 21st century.

3.2. Comparison of regional observed and future climate changes over croplands

To further assess the impacts of agrometeorological extremes on croplands, we utilised ERA5land and CMIP6 models to extract the regional averages of eight agrometeorological indicators over croplands for each year between 1955 and 2100. Then, we examine the recent trends and variations in agrometeorological extremes by comparing the regional averages of indicators derived from ERA5land data with those estimated from CMIP6 models (Fig. 3).

ERA5land indicates significant increasing trends in the Maximum heat intensity and number of W95/H95 events over the croplands between 1955 and 2014 in the southern Mediterranean region (Figs. 3a, f). ERA5land also shows significant decreasing trends in the maximum frost intensity, number of W95/C5, and D5/C5 events (Figs. 3c, g, h). However, the ERA5land does not show significant trends in drought intensity, extreme precipitation intensity, and the number of D5/H95 events (Figs. 3b, d, e).

In bias-corrected CMIP6 models, we note increasing trends in maximum heat intensity, maximum drought intensity and the number of D5/H95 and W95/H95 days (Figs. 3a-b, e-f). We also note decreasing trends in maximum frost intensity and the number of W95/C5 and D5/C5 days from 1955 to 2014 (Figs. 3c, g, h). However, over the historical period, most of the CMIP6 models do not indicate significant trends in maximum extreme precipitation intensity (Fig. 3d). These results indicate that, apart from drought intensity and the number of D5/H95 days, simulated historical trends align with ERA5land data.

However, there are significant differences in the magnitude of the projected trends across bias-corrected CMIP6 models. For instance, CanESM5 shows more pronounced trends in Maximum heat intensity while indicating less pronounced trends in the frequency of D5/C5 events (Figs. 3a, h). GISS-E2–1-G demonstrates the least pronounced trends in the maximum drought intensity and the number of extreme W95/C5 (Figs. 3b, g). FGOALS-g3 reveals less pronounced trends in Maximum heat intensity and the number of extreme D5/H95 events (Figs. 3a, e). Furthermore, UKESM1–0-LL shows more pronounced trends in maximum drought intensity and the number of extreme D5/H95 events (Figs. 3b, e). Meanwhile, CNRM-ESM2–1 exhibits less pronounced trends in maximum frost intensity and the number of W95/H95 events (Figs. 3c, f).

3.3. ToE in individual climatic stressors impacting croplands

This section delves into the ToE of significant changes in the maximum intensity of individual agrometeorological extremes. While we calculate the ToE for all agrometeorological indicators, the results for

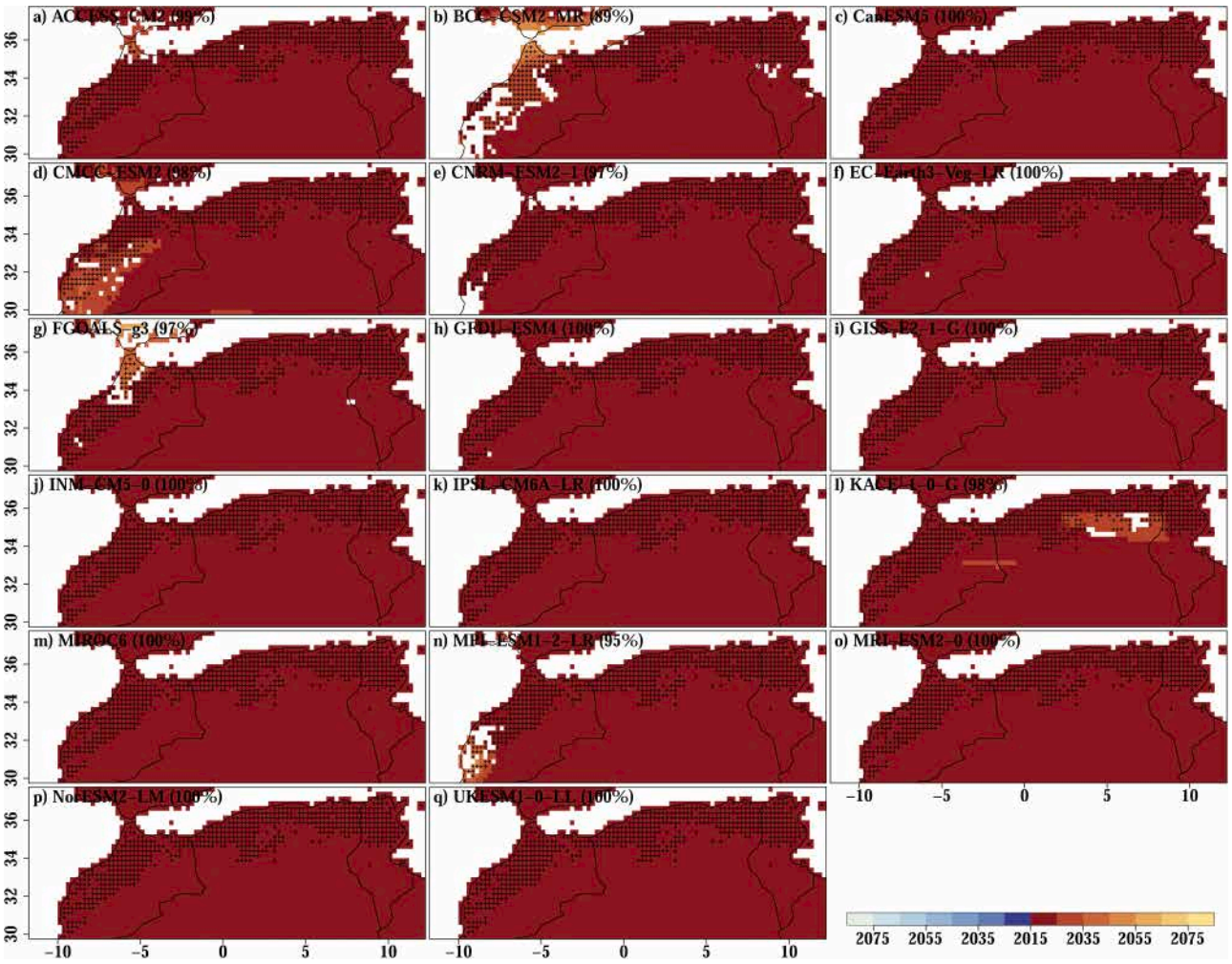

Fig. 7. Spatial and temporal distributions of ToE for the number of compound extreme dry and hot (D5/H95) events in 17 bias-corrected CMIP6 models under the SSP370 scenario over the southern Mediterranean region. For all models (**a**-q), red (blue) shades show ToE for significant increases (decreases) in the number of compound D5/H95 compared to the reference period (1995–2014). Plus (+) signs show the locations of croplands where the median of projected agrometeorological indicators significantly differs from the median of the historical period based on the Wilcoxon test at a 95 % confidence level. Numbers in parentheses indicate the percentage (%) of croplands that could be impacted by significant increases in the number of compound D5/H95 events by the end of the 21st century.

extreme precipitation are not discussed here, because the climate models do not project any significant trends in the southern Mediterranean region (cf. Sup. Mat. Fig. S1).

3.3.1. *Maximum heat intensity*

We analyse ToE of significant changes in maximum heat intensity across the southern Mediterranean region throughout the 21st century. We compare projections from 17 bias-corrected CMIP6 models under the SSP370 scenario with historical conditions from 1995 to 2014 (Fig. 4). Results indicate a significant increase in maximum heat intensity, projected to emerge by 2030 over an extensive area, potentially impacting around 93 % of the croplands by the end of the 21st century (Fig. 4). Notably, earlier emergence of stronger heat stress is expected in areas bordering the Sahara, while coastal regions may experience them later in the century (Fig. 4).

However, regarding the ToE and the extent of cropland areas that could be affected by significant increases in maximum heat intensity, we note substantial discrepancies from one CMIP6 model to another. CanESM5 and KACE-1–0-G present more pessimistic scenarios (Figs. 4c, l), with significant increases in maximum heat intensity emerging in the early 21st century and could potentially affect 100 % of croplands by 2100. In contrast, EC-Earth3-Veg-LR projects a later ToE (ca. 2080; Fig. 4f) of increased maximum heat intensity, which could affect 81 % of croplands by the end of the 21st century.

3.3.2. *Maximum drought intensity*

We now assess the ToE of significant changes in maximum drought intensity across the southern Mediterranean (Fig. 5). Most of the region is projected to experience significant increases in maximum drought intensity throughout the 21st century, according to bias-corrected CMIP6 models (Fig. 5). Croplands bordering the Sahara are expected to face increased maximum drought intensity as early as the beginning of the 21st century, while coastal regions will likely experience this significant increase later in the century (Fig. 5). In addition, an average of 52 % of croplands are projected to be impacted by this heightened drought intensity by the end of the 21st century (Fig. 5). Interestingly, a decrease in maximum drought intensity is projected for a small fraction of the coastal region of Morocco, Algeria, and Tunisia (ca. 9 % of croplands) in some CMIP6 models (e.g., CanESM5, FGOALS-g3, GISS-E2–1-G, INM-CM5–0, NorESM2-LM; Figs. 5c, g, i, j, p).

Furthermore, there are variations in the ToE and the extent of projected changes in maximum drought intensity from one CMIP6 model to another. For example, CMCC-ESM2, KACE-1–0-G, and MRI-ESM2–0 models project an earlier emergence (by 2030) of significant drought impacts on croplands (Figs. 5d, l, o). In contrast, the CNRM-ESM2–1 model suggests a later emergence (ca. 2080; Fig. 5e). Similarly, IPSL-

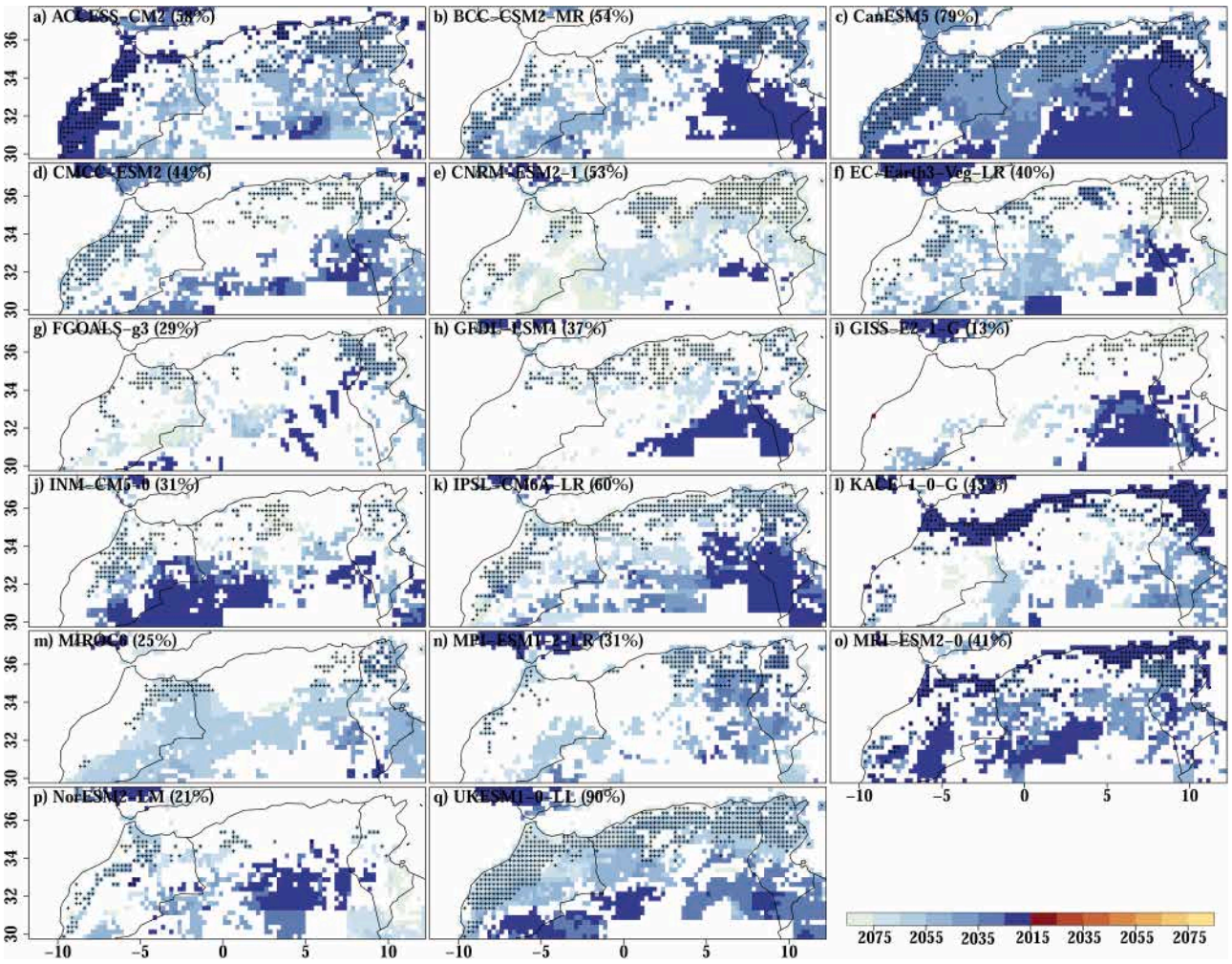

Fig. 8. Spatial and temporal distributions of ToE for the number of compound extreme wet and cold (W95/C5) events in 17 bias-corrected CMIP6 models under the SSP370 scenario over the southern Mediterranean region. For all models (**a**-q), red (blue) shades show ToE for significant increases (decreases) in the number of compound W95/C5 events compared to the reference period (1995–2014). Plus (+) signs show the locations of croplands where the median of projected agro-meteorological indicators significantly differs from the median of the historical period based on the Wilcoxon test at a 95 % confidence level. Numbers in parentheses indicate the percentage (%) of croplands that could be impacted by significant decreases in the number of compound W95/C5 events by the end of the 21st century.

CM6A-LR projects more widespread increases in maximum drought intensity, affecting 72 % of croplands by 2100 (Fig. 5k). Meanwhile, in GISS-E2–1-G, a significant increase in maximum drought intensity could affect a smaller fraction of croplands by 2100 (23 %; Fig. 5i).

3.3.3. *Maximum frost intensity*

We now investigate the spatiotemporal distribution of the ToE of significant changes in maximum frost intensity (Fig. 6). CMIP6 models consistently project significant decreases in maximum frost intensity in the early 21st century. Such changes are particularly found in the mountainous and arid regions of Morocco, as well as most of Algeria and Tunisia, which could affect an average of 47 % of croplands by 2100 (Fig. 6). However, it is important to note that, in most CMIP6 models, no significant changes in maximum frost intensity are projected for Moroccan coastal regions (Fig. 6).

Nevertheless, the ToE and the impacts of significant reductions in maximum frost intensity over croplands vary across different CMIP6 models. CanESM5 projects an earlier emergence of this decrease (ca. 2016) compared to EC-Earth3-Veg-LR (ca. 2038; Figs. 6c, f). Similarly, CanESM5 projects more widespread impacts on croplands (ca. 66 %), compared to MRI-ESM2–0 (ca. 26 %) by the end of the 21st century (Figs. 6c, o).

3.4. *ToE in compound agrometeorological stressors impacting croplands*

Here, we investigate the ToE of significant changes in the frequency of concurrent agrometeorological extremes using the same bias-corrected CMIP6 models under the SSP370 scenario. We do not discuss the results for W95/H95 events, as most CMIP6 models do not project significant changes over croplands (cf. Sup. Mat. Fig. S2).

3.4.1. *Number of extreme compound D5/H95 events*

We analyse the spatial and temporal distribution of the ToE of significant changes in the frequency of D5/H95 events. While all CMIP6 models consistently project an increase in D5/H95 days at the very beginning of the 21st century (ca. 2016–2020), it is important to note that there are some variations in their impacts on croplands. BCC—CSM2-MR suggests that approximately 89 % of croplands could be affected by increased frequency of D5/H95 events (Fig. 7b), whereas the majority of the CMIP6 models project a larger impact on around 100 % of croplands by the end of the 21st century (Fig. 7).

3.4.2. *Number of extreme compound W95/C5 events*

Our analysis of the frequency of compound W95/C5 events reveals a consistent decrease across all CMIP6 models. This decrease is projected to emerge around 2040 on average across all CMIP6 models and could

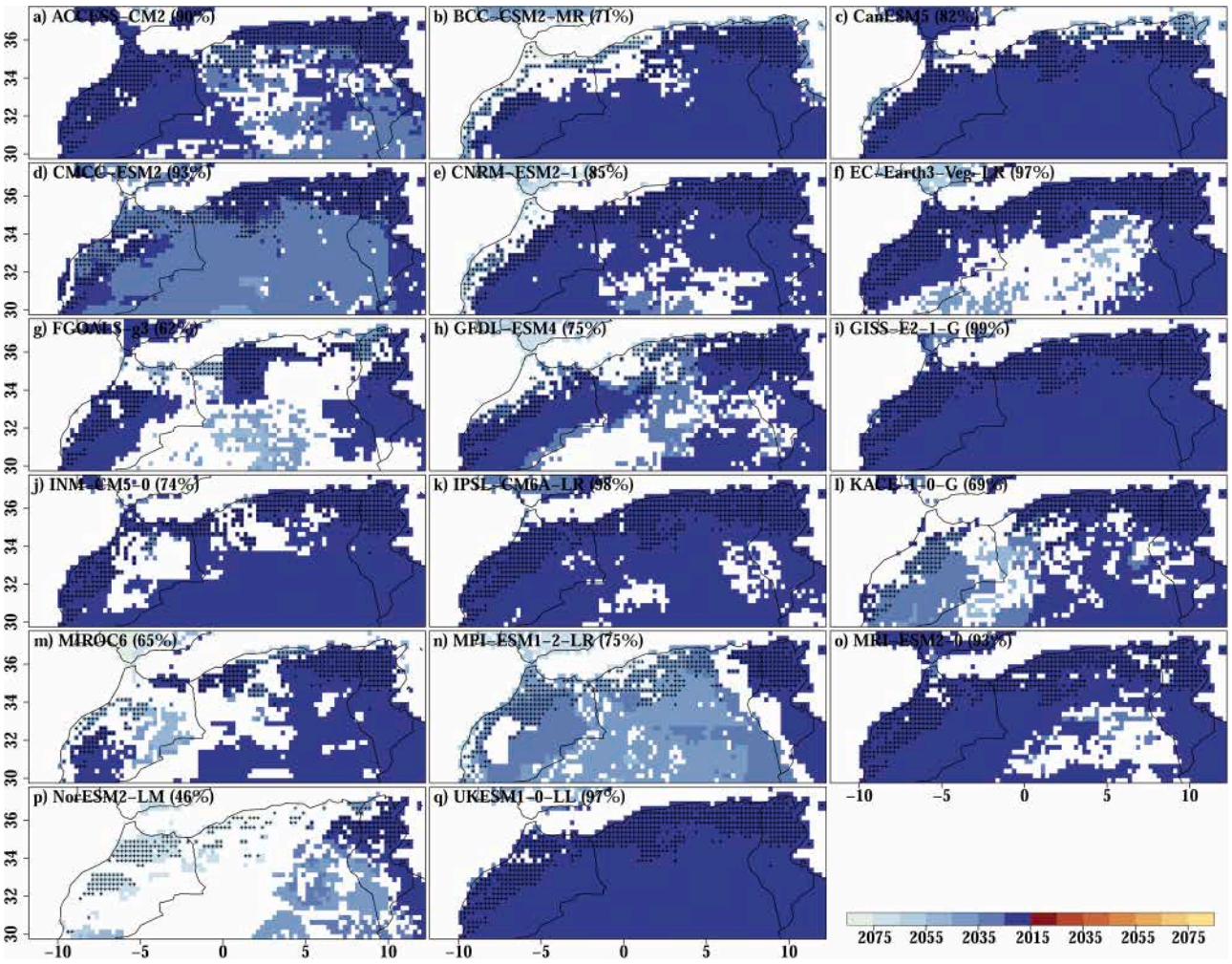

Fig. 9. Spatial and temporal distributions of ToE for the number of compound extreme dry and cold (D5/C5) events in 17 bias-corrected CMIP6 models under the SSP370 scenario over the southern Mediterranean region. For all models (**a**-q), red (blue) shades show ToE for significant increases (decreases) in the number of compound D5/C5 events compared to the reference period (1995–2014). Plus (+) signs show the locations of croplands where the median of projected agro-meteorological indicators significantly differs from the median of the historical period based on the Wilcoxon test at a 95 % confidence level. Numbers in parentheses indicate the percentage (%) of croplands that could be impacted by significant decreases in the number of compound D5/C5 events by the end of the 21st century.

impact an average of 44 % of the croplands by the end of the 21st century (Fig. 8). However, there is variation among the models regarding the timing and extent of these changes. For instance, FGOALS-g3 projects a later ToE (ca. 2068) compared to MRI-ESM2–0 (ca. 2024; Figs. 8g, o). Additionally, in GISS-E2–1-G, only 13 % of croplands are likely affected by such changes in the frequency of W95/C5 events during the 21st century, compared to UKESM1–0-LL, in which projected changes could affect up to 90 % of croplands (Figs. 8i, q).

3.4.2. *Number of extreme compound D5/C5 events*

We examine the ToE for changes in the frequency of compound D5/C5 events. All CMIP6 models project a consistent decline, which is expected to emerge around 2026, and could affect an average of 81 % of croplands by 2100 (Fig. 9). However, we note some variations across CMIP6 models. NorESM2-LM shows later ToE of a significant decrease in the frequency of D5/C5 events over the region (ca. 2052), and such decreases are projected to emerge even later (ca. 2080) in northern Morocco (Fig. 9p). In the same model, projected decreases in the frequency of D5/C5 also affect a smaller fraction of croplands (ca. 46 %) by the end of the 21st century (Fig. 9p). In contrast, GISS-E2–1-G model projects earlier (ca. 2016) and more widespread decrease in D5/C5 days affecting approximately 99 % of croplands by 2100 (Fig. 9i).

3.5. *Changes in agrometeorological extremes during the reproductive phase of winter wheat*

We analyse the ToE of significant changes in maximum heat shocks, drought intensity, and frost intensity, alongside the occurrence of extremely dry and hot days, and dry and frost days during the reproductive stage of winter wheat growth, incorporating insights from various existing phenological calendars over the southern Mediterranean region. The reproductive phase, which includes booting, heading, flowering, milk development, and grain filling, is the most sensitive stage to climatic changes and mostly occurs between February and June in the southern Mediterranean region (Latiri et al., 2010; Ahmad et al., 2021; Epule et al., 2022). For simplicity, we summarise the results in a table displaying the earliest, mean, and latest regional ToE of significant changes in agrometeorological hazards for each individual model over the wheat-harvested areas (Fig. 10). However, the spatial distributions of those changes are provided in the supplementary material (cf. Sup. Mat. Fig. S3-S7).

All CMIP6 models project consistent increases in maximum heat intensity across the southern Mediterranean region during the reproductive phase of winter wheat (Figs. 10, S3). In inland wheatlands, significant increases in maximum heat intensity are projected to occur at the earliest stage of the 21st century (ca. 2015), while these changes are

GCMs	Max Heatwave Intensity (>30°C)			Max Drought Intensity (SPEI)			Max Frost Intensity (<-4°C)			Number of dry & hot days (<1mm & >30°C)			Number of dry & cold days (<1mm & <-4°C)		
	Earliest	Mean	Latest	Earliest	Mean	Latest	Earliest	Mean	Latest	Earliest	Mean	Latest	Earliest	Mean	Latest
ACCESS-CM2	2015	2025	2075	2023	2057	2080	2015	2034	2078	2015	2022	2075	2015	2027	2059
BCC-CSM2-MR	2015	2022	2042	2015	2055	2079	2015	2033	2065	2015	2019	2043	2015	2033	2065
CanESM5	2015	2015	2031	2015	2057	2080	2015	2016	2040	2015	2015	2031	2015	2016	2040
CMCC-ESM2	2015	2018	2026	2015	2054	2080	2015	2026	2038	2015	2016	2026	2015	2026	2038
CNRM-ESM2-1	2015	2023	2078	2015	2062	2080	2046	2069	2080	2015	2021	2078	2015	2039	2080
EC-Earth3-Veg-LR	2015	2025	2069	2015	2036	2079	2015	2046	2080	2015	2023	2069	2015	2028	2074
FGOALS-g3	2015	2018	2043	2015	2055	2080	2015	2023	2070	2015	2018	2043	2015	2029	2058
GFDL-ESM4	2015	2016	2025	2015	2051	2080	2015	2044	2073	2015	2015	2026	2015	2047	2071
GISS-E2-1-G	2015	2017	2025	2015	2039	2076	2015	2017	2042	2015	2015	2025	2015	2016	2042
INM-CM5-0	2015	2015	2043	2015	2042	2076	2015	2028	2056	2015	2015	2045	2015	2027	2056
IPSL-CM6A-LR	2015	2046	2076	2015	2033	2076	2015	2030	2072	2015	2035	2076	2015	2027	2060
KACE-1-0-G	2015	2016	2052	2015	2025	2080	2015	2024	2053	2015	2016	2064	2015	2033	2066
MIROC6	2015	2016	2062	2015	2034	2059	2015	2037	2080	2015	2016	2062	2015	2016	2041
MPI-ESM1-2-LR	2015	2024	2080	2015	2038	2075	2015	2038	2068	2015	2021	2080	2015	2026	2068
MRI-ESM2-0	2015	2029	2079	2015	2059	2080	2015	2042	2075	2015	2022	2079	2015	2021	2064
NorESM2-LM	2015	2015	2038	2015	2054	2078	2015	2028	2068	2015	2015	2038	2015	2022	2068
UKESM1-0-LL	2015	2019	2064	2015	2038	2079	2015	2040	2074	2015	2017	2064	2015	2040	2076
Mean	**2015**	**2021**	**2053**	**2015**	**2046**	**2077**	**2017**	**2034**	**2065**	**2015**	**2019**	**2054**	**2015**	**2028**	**2060**

Fig. 10. Range of Time of Emergence (ToE) for various extreme agrometeorological events during the reproductive phase of winter wheat growth using 17 bias-corrected CMIP6 models under the SSP370 scenario in the southern Mediterranean region. The blue/red shades indicate the expected ToE of decreased/increased changes compared to the reference period (1995–2014).

expected to emerge in the mid-term future (ca. 2053) in coastal wheatlands (Fig. S3). We also note non-negligible differences among models regarding the ToE of significant changes in maximum heat intensity. Some models like CanESM5, INM-CM5–0, and NorESM2-LM project earlier emergence of such changes, whereas IPSL-CM6A-LR projects a later emergence (Fig. 10). Similarly, CanESM5 projects a larger impact on wheatlands, with around 99 % affected by increased maximum heat intensity, while MRI-ESM2–0 suggests a much smaller fraction, impacting 40 % of the wheatlands (cf. Sup. Mat. Figs. S3c, o)

Similarly, CMIP6 models consistently project an increase in maximum drought intensity, with ToE varying during the 21st century (Figs. 10, S4). Nevertheless, CNRM-ESM2–1 projects a later mean ToE in 2062, while KACE-1–0-G suggests an earlier ToE by 2025 over the wheat-harvested areas (Fig. 10). Additionally, the projected drought impacts on wheatlands are found to affect a smaller fraction of wheatlands compared to heatwaves (cf. Fig. S4). IPSL-CM6A-LR suggests that 59 % of wheatlands could be affected by increased drought intensity, whereas GFDL-ESM4 projects an even smaller area, impacting 31 % of the wheatlands (Figs. S4h, k).

Maximum frost intensity is projected to significantly decrease during the reproductive phase of winter wheat, with an average ToE in the mid-term (ca. 2034; Figs. 10, S5). These changes are expected to emerge earlier (ca. 2016) in CanESM5, while CNRM-ESM2–1 shows later ToE (ca. 2069) over the wheat-harvested areas (Fig. 10). However, we note that these changes could only affect a very small fraction of wheatland areas (ca. 14 %) mostly located in the mountainous regions (cf. Fig. S5).

Regarding the frequency of extreme compound events during the same phenological stage of winter wheat, the number of extremely dry and hot days is projected to significantly increase, with an average ToE in the near-term future (ca. 2019; Figs. 10, S6). Again, there are variations in the extent of impacts and timing of emergence among CMIP6 models. In CanESM5, up to 100 % of wheatlands could be affected by increased frequency of compound dry and hot days, while only 39 % of wheatlands could be affected according to CNRM-ESM2–1 projection (Figs. S6c, e). Conversely, extremely dry and cold days are projected to become less frequent, with a ToE in the near-term future (ca. 2028; Figs. 10, S7). However, these decreases are projected to affect only a minor proportion (ca. 7 %) of wheat-growing areas (Fig. S7).

3.6. *Cumulative negative and positive impacts of agrometeorological hazards*

In this section, we evaluate the potential cumulative positive and negative impacts of various agrometeorological extremes on croplands and wheatlands in the near-term (by 2030), mid-term (by 2050), and long-term (by 2100) future. Here, a negative (positive) impact is defined as a significant change in agrometeorological extremes that is likely to hamper (enhance) crop productivity (cf. Tables 2-3).

In the near-term outlook (by 2030), our analysis reveals that between two and six changes in agrometeorological extremes could negatively impact croplands and wheatlands (Fig. 11a). During the same period, coastal regions will potentially be affected by fewer negative agrometeorological impacts compared to inland regions (Fig. 11a). In particular, up to 53 % (47 %) of croplands could be affected by two (three) negative agrometeorological impacts during this period of the 21st century, while 68 % (29 %) of wheatlands are likely to be affected by four (five) cumulative negative impacts (Figs. 12a-b). Moreover, fewer potential positive agrometeorological impacts are found over croplands and wheatlands in the near-term future (Fig. 11b). Up to 98 % of croplands and 95 % of wheatlands might experience one or two positive cumulative changes in agrometeorological hazards by 2030 (Figs. 12a-b). Additionally, up to 4 % of Wheatlands will probably experience three cumulative positive impacts by 2030 (Fig. 12b). These potential positive climate impacts are more pronounced in Algeria compared to Morocco and Tunisia (Fig. 11b).

The mid-term projection (by 2050) suggests a potential increase in

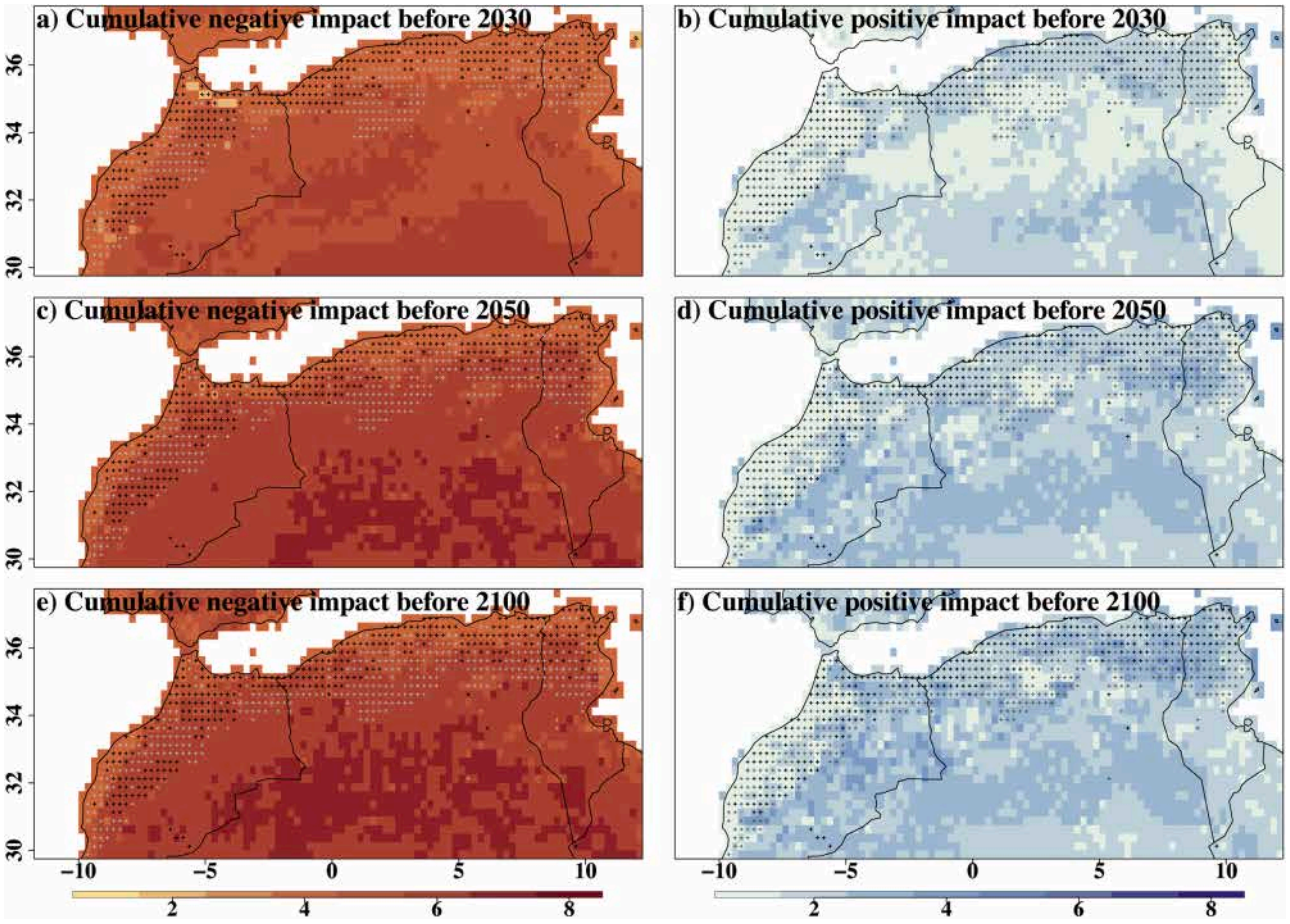

Fig. 11. Spatial distribution of the cumulative positive and negative impacts associated with projected changes in agrometeorological extremes across the southern Mediterranean region, based on the multi-model mean of bias-corrected CMIP6 models under the SSP370 scenario. **a**-b) show the potential cumulative negative (left) and positive (right) agrometeorological impacts before 2030. **c**-f) same representation but by 2050 and 2100. Black and grey plus (+) signs show the locations of wheatlands and other croplands, respectively.

negative agrometeorological impacts (up to six) over croplands and wheatlands (Fig. 11c). Like the near-term outlook, cultivated regions bordering the Sahara are expected to be more exposed. However, exposure to negative agrometeorological extremes gradually decreases towards the coastal areas (Fig. 11c). While the proportion of cultivated areas experiencing three negative agrometeorological impacts is projected to increase to 82 % in croplands, the possibility of six negative agrometeorological impacts is projected to emerge in over 34 % of wheatlands by 2050 (Figs. 12a-b). Positive agrometeorological impacts remain limited in the mid-term future (Fig. 11d). These positive changes are more pronounced in Algeria and Tunisia than in Morocco. Up to 72 % of croplands and 70 % of wheatlands are projected to experience between two and three positive agrometeorological impacts by 2050 (Fig. 12a-b).

By 2100, more severe agrometeorological conditions are projected, with an extended domain affected by multiple negative impacts (up to seven) over croplands and wheatlands (Fig. 11e). This increased exposure is expected to be more pronounced in coastal areas, where higher cumulative negative impacts are projected compared to previous outlooks (Fig. 11e). In the long-term future, most croplands (up to 83 %) could face three negative agrometeorological impacts, while 40 % of wheatlands are projected to be affected by six negative agrometeorological impacts (Figs. 12a-b). Furthermore, three positive agrometeorological impacts are projected over 35 % of croplands (Fig. 12a). Such increases in the number of potential positive agrometeorological impacts are also found over wheatlands which are expected to experience similar cumulative positive impacts, with a minor increase in the possibility of four cumulative positive impacts (Fig. 12b).

4. Discussion and conclusion

Feeding a globally growing population is becoming increasingly challenging due to the present and projected climatic extremes disrupting crop production, especially in the Global South (IPCC, 2022). To enable communities to adapt and meet their long-term objectives for food security, we need to further understand future climate trends and their potential impacts on agricultural areas (IPCC, 2022). Here, we used bias-corrected CMIP6 models under the SSP370 scenario to investigate potential future changes in agrometeorological extremes across croplands and wheatlands in the southern Mediterranean region.

Our findings reveal that the cultivated lands in the southern Mediterranean region could experience between four and seven negative changes in agrometeorological extremes during the 21st century. Higher exposure to negative agrometeorological impacts is projected for the agricultural lands bordering the Sahara compared to coastal regions. Across all CMIP6 models, these negative agrometeorological impacts include a consistent increase in maximum heat and drought intensities, projected to emerge primarily by the near- and mid-term future (by 2030 and 2050) over croplands and wheatlands. Such increased heat intensity poses significant risks to crop production, as they could affect various physiological and metabolic processes within different phases of crop development (del Pozo et al., 2019; Zhu et al., 2021). For instance, extreme temperatures can reduce photosynthesis rates, increase water demands, and amplify the vulnerability of crops to diseases and pest

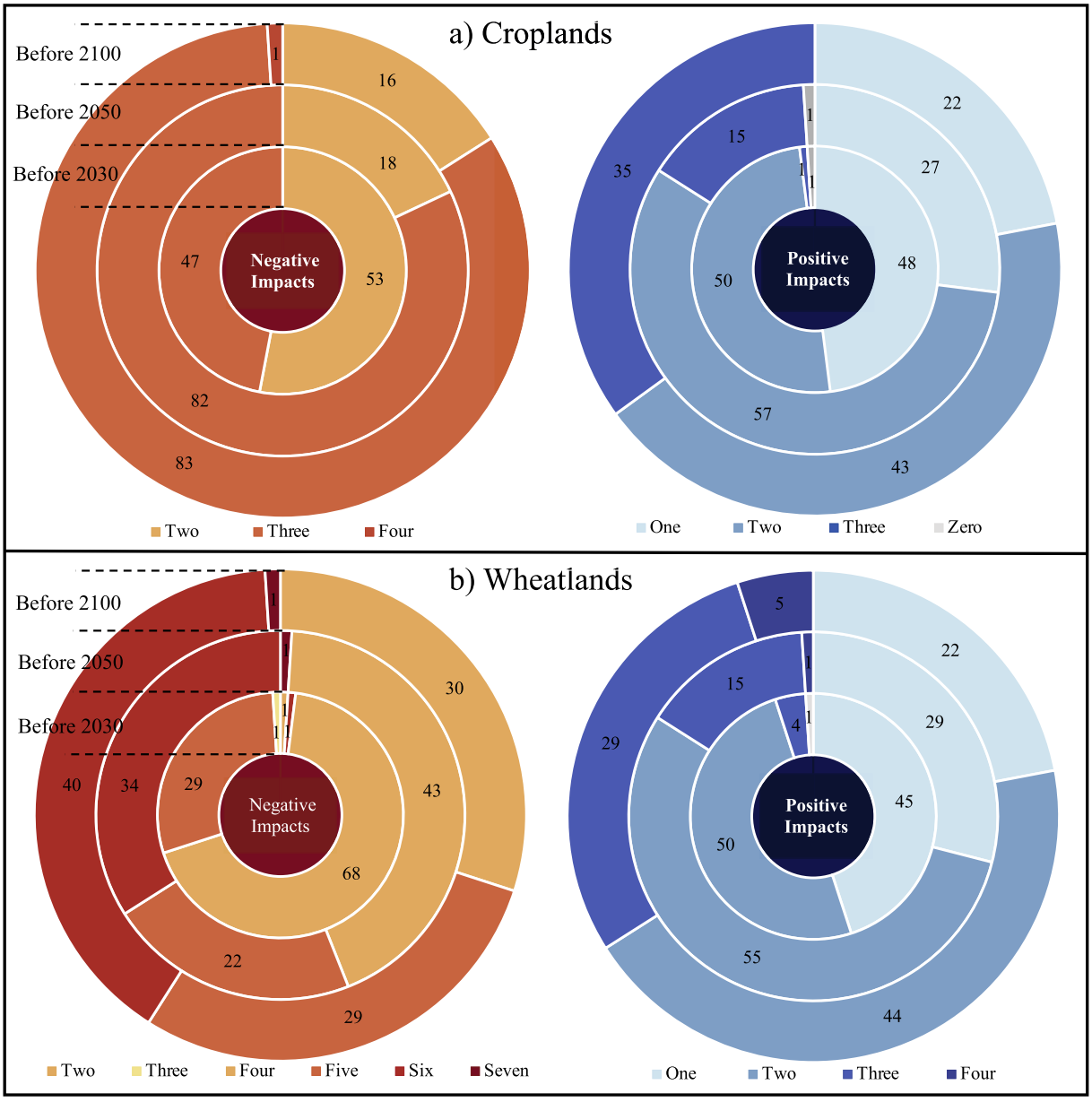

Fig. 12. The potential cumulative negative (left) and positive (right) impacts of climate change over the (a) Croplands and (b) Wheatlands across three timeframes: near-term (by 2030), mid-term (by 2050), and long-term (by 2100). The numbers in the figure show the percentage of crops which would be potentially affected by different cumulative impacts.

infestations, ultimately lowering crop yield and quality (Lizaso et al., 2018; Rashid et al., 2018; Skendžić et al., 2021; Alrteimei et al., 2022; Bernacchi et al., 2023). Similarly, increased drought lowers soil moisture content, hindering seed germination, root development, and nutrient uptake, leading to yield losses and decreased crop quality, particularly in rain-fed agricultural systems prevalent in the southern Mediterranean region (Hubbard et al., 2012; Bista et al., 2018; Licaj et al., 2023). Furthermore, we found an increase in the frequency of extreme compound D5/H95 days, which could emerge in the near-term future (by 2030) and exacerbate plant stress levels, potentially resulting in substantial yield losses (Heino et al., 2023). Such projected increased intensity and frequency of combined heat and drought stresses are consistent with previous work using CMIP3 and CMIP5 by Barcikowska et al. (2020). In addition, this study suggests that such changes could be driven by the diminishing role of local atmospheric dynamics and teleconnections and an increasing influence of warming land surface in maintaining temperature and precipitation balance in the southern Mediterranean.

In contrast, southern Mediterranean croplands are likely to encounter between one to four positive changes in agrometeorological impacts. These positive agrometeorological impacts are projected to emerge in the near- and mid-term future (by 2030 or 2050), with more pronounced effects over Algeria and western parts of Tunisia. Notably, our study reveals for the first time that, bias-corrected CMIP6 models consistently project a decrease in frost intensity and the frequency of W95/C5 and D5/C5 days. These reductions are important because they could mitigate frost damage and extend growing seasons in areas currently limited by frost risk (Abi Saab et al., 2019; Liu and Zhang, 2020). However, it is crucial to quantify the relative importance of these changes by integrating state-of-the-art CMIP6 models into crop models to fully understand the implications of these changes on crop production (Jägermeyr et al., 2021).

Furthermore, the implementation of adaptation strategies is essential to mitigate their negative impacts on crop production, particularly in the

near- and mid-term futures, when these extreme events are projected to emerge over agricultural areas in the southern Mediterranean region (Abbas et al., 2023). In the Mediterranean context, where most current cultivars have been used under high resource input conditions, it is crucial to develop new cultivars with higher potential yields adapted to water-limiting and high-temperature conditions (del Pozo et al., 2019). Moreover, adjusting the sowing dates according to the new climate conditions can potentially mitigate the adverse impacts of extreme events on agricultural production by enabling the crops to develop ahead of the occurrence of extreme events (Baum et al., 2020).

Additionally, to prevent the degradation of soil and water resources of the region, applying other efficient agronomical practices, such as prioritizing the use of available water, transitioning from traditional irrigation systems to modern methods, and adopting no-tillage and minimum-tillage systems, can be implemented (Zalidis et al., 2002; Lampurlanés et al., 2016). However, to ensure the long-term viability and effectiveness of the potential adaptation strategies for future decades, evaluating them within crop models under future climate change scenarios is crucial (Grigorieva et al., 2023). This approach of stress-testing how well adaptation strategies perform under future climate conditions could offer insightful information for long-term, sustainable decision-making in the agricultural sectors of the southern Mediterranean region.

CRediT authorship contribution statement

Behnam Mirgol: Writing – review & editing, Writing – original draft, Visualization, Validation, Software, Methodology, Investigation, Formal analysis, Conceptualization. **Bastien Dieppois:** Writing – review & editing, Visualization, Validation, Supervision, Project administration, Methodology, Funding acquisition, Conceptualization. **Jessica Northey:** Writing – review & editing, Supervision, Funding acquisition, Conceptualization. **Jonathan Eden:** Writing – review & editing, Supervision, Funding acquisition, Conceptualization. **Lionel Jarlan:** Writing – review & editing, Supervision, Methodology, Conceptualization. **Saïd Khabba:** Writing – review & editing, Supervision, Methodology, Conceptualization. **Michel Le Page:** Writing – review & editing, Supervision, Methodology, Conceptualization. **Gil Mahe:** Writing – review & editing, Supervision, Methodology, Conceptualization.

Declaration of competing interest

The authors declare that they have no known competing financial interests or personal relationships that could have appeared to influence the work reported in this paper.

Data availability

Data will be made available on request.

Acknowledgements

The authors would like to thank Coventry University, United Kingdom for funding this PhD Studentship titled “Assessing the impacts of climate change on agricultural productivity and practices in the southern Mediterranean region”, through GCRF scheme.

Supplementary materials

Supplementary material associated with this article can be found, in the online version, at doi:10.1016/j.agrformet.2024.110232.

References

Abbas, A., Bhatti, A.S., Ullah, S., Ullah, W., Waseem, M., Zhao, C., Dou, X., Ali, G., 2023 Mar. Projection of precipitation extremes over South Asia from CMIP6 GCMs. J. Arid. Land 15 (3), 274–296. https://doi.org/10.1007/s40333-023-0050-3.

Abd-Elmabod, S.K., Jordán, A., Fleskens, L., Phillips, J.D., Muñoz-Rojas, M., van der Ploeg, M., Anaya-Romero, M., El-Ashry, S., de la Rosa, D., 2017 Jan 1. Modeling agricultural suitability along soil transects under current conditions and improved scenario of soil factors. Soil Mapp. Process Model. Sustain. Land Use Manag 193–219. https://doi.org/10.1016/B978-0-12-805200-6.00007-4.

Abd-Elmabod, S.K., Muñoz-Rojas, M., Jordán, A., Anaya-Romero, M., Phillips, J.D., Jones, L., Zhang, Z., Pereira, P., Fleskens, L., van Der Ploeg, M., de la Rosa, D., 2020 Sep 1. Climate change impacts on agricultural suitability and yield reduction in a Mediterranean region. Geoderma 374, 114453. https://doi.org/10.1016/j.geoderma.2020.114453.

Abi Saab, M.T., Houssemeddine Sellami, M., Giorio, P., Basile, A., Bonfante, A., Rouphael, Y., Fahed, S., Jomaa, I., Stephan, C., Kabalan, R., Massaad, R, 2019 July 17. Assessing the potential of cereal production systems to adapt to contrasting weather conditions in the Mediterranean region. Agronomy 9 (7), 393. https://doi.org/10.3390/agronomy9070393.

Ahmad, Q.U., Biemans, H., Moors, E., Shaheen, N., Masih, I., 2021 Jan. The impacts of climate variability on crop yields and irrigation water demand in South Asia. Water (Basel) 13 (1), 50. https://doi.org/10.3390/w13010050.

Alrteimei, H.A., Ash'aari, Z.H., Muharram, F.M., 2022 Oct 28. Last decade assessment of the impacts of regional climate change on crop yield variations in the Mediterranean region. Agriculture 12 (11), 1787. https://doi.org/10.3390/agriculture12111787.

Antonelli M., Basile L., Gagliardi F., Isernia P. The future of the Mediterranean agri-food systems: trends and perspectives from a Delphi survey. *Land Use Policy*. 2022 Sep 1; 120:106263. https://doi.org/10.1016/j.landusepol.2022.106263.

Awika, J.M., 2011. Major cereal grains production and use around the world. InAdvances in Cereal science: Implications to Food Processing and Health Promotion. American Chemical Society, pp. 1–13. https://doi.org/10.1021/bk-2011-1089.ch001.

Barcikowska M.J., Kapnick S.B., Krishnamurty L., Russo S., Cherchi A., Folland C.K. Changes in the future summer Mediterranean climate: contribution of teleconnections and local factors. *Earth Syst. Dynamics*. 2020 Feb 18;11(1):161–181. https://doi.org/10.5194/esd-11-161-2020.

Barlow K.M., Christy B.P., O'Leary G.J., Riffkin P.A., Nuttall J.G. Simulating the impact of extreme heat and frost events on wheat crop production: a review. *Field Crops Res.*. 2015 Feb 1;171:109–19. https://doi.org/10.1016/j.fcr.2014.11.010.

Barnabás, B., Jäger, K., Fehér, A., 2008 Jan. The effect of drought and heat stress on reproductive processes in cereals. Plant Cell Environ. 31 (1), 11–38. https://doi.org/10.1111/j.1365-3040.2007.01727.x.

Baum, M.E., Licht, M.A., Huber, I., Archontoulis, S.V., 2020 Sep 1. Impacts of climate change on the optimum planting date of different maize cultivars in the central US Corn Belt. Europ. J. Agron. 119, 126101 https://doi.org/10.1016/j.eja.2020.126101.

Benabdelkader M., Saifi R., Saifi H. Sustainable agriculture in some arab maghreb countries (Morocco, Algeria, Tunisia). Agro-environm. Sustain. MENA Regions. 2021:233–261. https://doi.org/10.1007/978-3-030-78574-1_10.

Bernacchi, C.J., Ruiz-Vera, U.M., Siebers, M.H., DeLucia, N.J., Ort, D.R., 2023 July 7. Short-and long-term warming events on photosynthetic physiology, growth, and yields of field grown crops. Biochem. J 480 (13), 999–1014. https://doi.org/10.1042/BCJ20220433.

Bi, D., Dix, M., Marsland, S., O'farrell, S., Sullivan, A., Bodman, R., Law, R., Harman, I., Srbinovsky, J., Rashid, H.A., Dobrohotoff, P, 2020 Oct 8. Configuration and spin-up of ACCESS-CM2, the new generation Australian community climate and earth system simulator coupled model. J. Southern Hemisph Earth Syst. Sci 70 (1), 225–251. https://doi.org/10.1071/ES19040.

Bista D.R., Heckathorn S.A., Jayawardena D.M., Mishra S., Boldt J.K. Effects of drought on nutrient uptake and the levels of nutrient-uptake proteins in roots of drought-sensitive and-tolerant grasses. *Plants*. 2018 Mar 30;7(2):28. https://doi.org/10.3390/plants7020028.

Bouabdelli, S., Zeroual, A., Meddi, M. and Assani, A., 2022. Impact of temperature on agricultural drought occurrence under the effects of climate change. *Theor. Appl. Climatol.*, 148(1), pp.191–209. https://doi.org/10.1007/s00704-022-03935-7.

Bouchemal, S., 2021. A note on the dynamics of food systems in Algeria: the example of the Ziban and the Souf. World J. Adv. Res. Rev 10 (1), 048–055. https://doi.org/10.30574/wjarr.2021.10.1.0124.

Boucher, O., Servonnat, J., Albright, A.L., Aumont, O., Balkanski, Y., Bastrikov, V., Bekki, S., Bonnet, R., Bony, S., Bopp, L., Braconnot, P., Brockmann, P., Cadule, P., Caubel, A., Cheruy, F., Codron, F., Cozic, A., Cugnet, D., D'Andrea, F., Davini, P., de Lavergne, C., Denvil, S., Deshayes, J., Devilliers, M., Ducharne, A., Dufresne, J.-L., Dupont, E., Éthé, C., Fairhead, L., Falletti, L., Flavoni, S., Foujols, M.-A., Gardoll, S., Gastineau, G., Ghattas, J., Grandpeix, J.-Y., Guenet, B., Lionel, Guez E, Guilyardi, E., Guimberteau, M., Hauglustaine, D., Hourdin, F., Idelkadi, A., Joussaume, S., Kageyama, M., Khodri, M., Krinner, G., Lebas, N., Levavasseur, G., Lévy, C., Li, L., Lott, F., Lurton, T., Luyssaert, S., Madec, G., Madeleine, J.-B., Maignan, F., Marchand, M., Marti, O., Mellul, L., Meurdesoif, Y., Mignot, J., Musat, I., Ottlé, C., Peylin, P., Planton, Y., Polcher, J., Rio, C., Rochetin, N., Rousset, C., Sepulchre, P., Sima, A., Swingedouw, D., Thiéblemont, R., Traore, A.K., Vancoppenolle, M., Vial, J., Vialard, J., Viovy, N., Vuichard, N, 2020 Jul. Presentation and evaluation of the IPSL-CM6A-LR climate model. J. Adv. Model. Earth Syst 12 (7), e2019MS002010. https://doi.org/10.1029/2019MS002010.

Bouras E., Jarlan L., Khabba S., Er-Raki S., Dezetter A., Sghir F., Tramblay Y. Assessing the impact of global climate changes on irrigated wheat yields and water

requirements in a semi-arid environment of Morocco. *Sci. Rep*. 2019 Dec 16;9(1): 19142. https://doi.org/10.1038/s41598-019-55251-2.
Cammarano, D., Ceccarelli, S., Grando, S., Romagosa, I., Benbelkacem, A., Akar, T., Al-Yassin, A., Pecchioni, N., Francia, E., Ronga, D., 2019 May 1. The impact of climate change on barley yield in the Mediterranean basin. Europ. J. Agron 106, 1. https://doi.org/10.1016/j.eja.2019.03.002.
Chen G., Li X., Liu X. Global land projection based on plant functional types with a 1-km resolution under socio-climatic scenarios. *Sci. Data*. 2022 Mar 30;9(1):125. https://doi.org/10.1038/s41597-022-01208-6.
Cheong, B.E., Ho, W.W., Biddulph, B., Wallace, X., Rathjen, T., Rupasinghe, T.W., Roessner, U., Dolferus, R., 2019 Nov. Phenotyping reproductive stage chilling and frost tolerance in wheat using targeted metabolome and lipidome profiling. Metabolomics 15 (11), 1–9. https://doi.org/10.1007/s11306-019-1606-2.
Chourghal N., Lhomme J.P., Huard F., Aidaoui A. Climate change in Algeria and its impact on durum wheat. Regional environmental change. 2016 Aug;16:1623–34. https://doi.org/10.1007/s10113-015-0889-8.
Cramer, W., Guiot, J., Fader, M., Garrabou, J., Gattuso, J.P., Iglesias, A., Lange, M.A., Lionello, P., Llasat, M.C., Paz, S., Peñuelas, J., 2018 Nov. Climate change and interconnected risks to sustainable development in the Mediterranean. Nat. Clim. Chang 8 (11), 972–980. https://doi.org/10.1038/s41558-018-0299-2.
del Pozo A., Brunel-Saldias N., Engler A., Ortega-Farias S., Acevedo-Opazo C., Lobos G. A., Jara-Rojas R., Molina-Montenegro M.A. Climate change impacts and adaptation strategies of agriculture in Mediterranean-climate regions (MCRs). *Sustainability*. 2019 May 15;11(10):2769. https://doi.org/10.3390/su11102769.
Deryng D., Elliott J., Folberth C., Müller C., Pugh T.A., Boote K.J., Conway D., Ruane A. C., Gerten D., Jones J.W., Khabarov N. Regional disparities in the beneficial effects of rising CO2 concentrations on crop water productivity. *Nat. Clim. Chang*. 2016 Aug; 6 (8):786–790. https://doi.org/10.1038/nclimate2995.
Dias, A.S., Lidon, F.C., 2009 Apr. Evaluation of grain filling rate and duration in bread and durum wheat, under heat stress after anthesis. J. Agron. Crop Sci 195 (2), 137–147. https://doi.org/10.1111/j.1439-037X.2008.00347.x.
Döscher R., Acosta M., Alessandri A., Anthoni P., Arsouze T., Bergman T., Bernardello R., Boussetta S., Caron L-P, Carver G., Castrillo M., Catalano F., Cvijanovic I., Davini P., Dekker E., Doblas-Reyes F.J., Docquier D., Echevarria P., Fladrich U., Fuentes-Franco R., Gröger M. v. Hardenberg J., Hieronymus J., Karami M.P., Keskinen J.-.P., Koenigk T., Makkonen R., Massonnet F., Ménégoz M., Miller P.A., Moreno-Chamarro E., Nieradzik L., van Noije T., Nolan P., O'Donnell D., Ollinaho P., van den Oord G., Ortega P., Prims O.T., Ramos A., Reerink T., Rousset C., Ruprich-Robert Y., Le Sager P., Schmith T., Schrödner R., Serva F., Sicardi V., Sloth Madsen M., Smith B., Tian T., Tourigny E., Uotila P., Vancoppenolle M., Wang S., Wårlind D., Willén U., Wyser K., Yang S., Yepes-Arbós X., Zhang Q. The EC-Earth3 earth system model for the coupled model intercomparison project 6. *Geosci. Model Devel*. 2021 Feb 11; 15(7): 1–90. https://doi.org/10.5194/gmd-15-2973-2022.
Droogers P., Allen R.G. Estimating reference evapotranspiration under inaccurate data conditions. *Irrigat. Drainage Syst.*, 2002; 16(1): 33–45. https://doi.org/10.1023/A:1015508322413.
Epule T.E., Chehbouni A., Dhiba D., Etongo D., Achli S., Salih W., Er-Raki S. Identifying gaps in actual and simulated/potential yield and growing season precipitation in Morocco. Environmental Science and Pollution Research. 2022 Dec; 29(56): 84844–60. https://doi.org/10.1007/s11356-022-21671-3.
Frederiks, T.M., Christopher, J.T., Sutherland, M.W., Borrell, A.K., 2015. Post-head-emergence frost in wheat and barley: defining the problem, assessing the damage, and identifying resistance. J. Exp. Bot. 66 (12), 3487–3498. https://doi.org/10.1093/jxb/erv088.
Gaaloul, N., Eslamian, S.A., Katlance, R., 2021 Feb 1. Impacts of climate change and water resources management in the southern Mediterranean countries. Water Product. J 1 (1), 51–72.
Gaetani M., Janicot S., Vrac M., Famien A.M., Sultan B. Robust assessment of the time of emergence of precipitation change in West Africa. Sci. Rep. 2020 May 6;10(1):7670. https://doi.org/10.1038/s41598-020-63782-2.
Giraldo, P., Benavente, E., Manzano-Agugliaro, F., Gimenez, E., 2019 July 3. Worldwide research trends on wheat and barley: a bibliometric comparative analysis. Agronomy 9 (7), 352. https://doi.org/10.3390/agronomy9070352.
Grigorieva, E., Livenets, A., Stelmakh, E., 2023 Oct 6. Adaptation of agriculture to climate change: a scoping review. Climate 11 (10), 202. https://doi.org/10.3390/cli11100202.
Guion A., Turquety S., Polcher J., Pennel R., Bastin S., Arsouze T. Droughts and heatwaves in the Western Mediterranean: impact on vegetation and wildfires using the coupled WRF-ORCHIDEE regional model (RegIPSL). Climate Dynamics. 2022 May; 58(9):2881–2903. https://doi.org/10.1007/s00382-021-05938-y.
Hamed, K.H., Rao, A.R., 1998 Jan 30. A modified Mann-Kendall trend test for autocorrelated data. J. Hydrol 204 (1–4), 182–196. https://doi.org/10.1016/S0022-1694(97)00125-X.
Hassan M.A., Xiang C., Farooq M., Muhammad N., Yan Z., Hui X., Yuanyuan K., Bruno A. K., Lele Z., Jincai L. Cold stress in wheat: plant acclimation responses and management strategies. *Front. Plant Sci*. 2021 Jul 8; 12:676884. https://doi.org/10.3389/fpls.2021.676884.
Hatfield J.L., Prueger J.H. Temperature extremes: effect on plant growth and development. Weather Climate Extrem. 2015 Dec 1;10:4–10. https://doi.org/10.1016/j.wace.2015.08.001.
Hawkins, E., Sutton, R., 2012 Jan. Time of emergence of climate signals. Geophys. Res. Lett 39 (1). https://doi.org/10.1029/2011GL050087.
He Y., Zhao Y., Sun S., Fang J., Zhang Y., Sun Q., Liu L., Duan Y., Hu X., Shi P. Global warming determines future increase in compound dry and hot days within wheat growing seasons worldwide. *Climat. Change*. 2024 Apr; 177(4):1–22. https://doi.org/10.1007/s10584-024-03718-1.
Heino M., Kinnunen P., Anderson W., Ray D.K., Puma M.J., Varis O., Siebert S., Kummu M. Increased probability of hot and dry weather extremes during the growing season threatens global crop yields. *Sci. Rep*. 2023 Mar 3; 13(1):3583. https://doi.org/10.1038/s41598-023-29378-2.
Horowitz, L.W., Naik, V., Paulot, F., Ginoux, P.A., Dunne, J.P., Mao, J., Schnell, J., Chen, X., He, J., John, J.G., Lin, M., 2020 Oct. The GFDL global atmospheric chemistry-climate model AM4. 1: model description and simulation characteristics. J. Adv. Model. Earth Syst 12 (10), e2019MS002032. https://doi.org/10.1029/2019MS002032.
Hu, P., Chapman, S.C., Sukumaran, S., Reynolds, M., Zheng, B., 2022 Jun 24. Phenological optimization of late reproductive phase for raising wheat yield potential in irrigated mega-environments. J. Exp. Bot. 73 (12), 4236–4249. https://doi.org/10.1093/jxb/erac144.
Hu, Z., Liu, S., Zhong, G., Lin, H., Zhou, Z., 2020 Oct 25. Modified Mann-Kendall trend test for hydrological time series under the scaling hypothesis and its application. Hydrol. Sci. J 65 (14), 2419–2438. https://doi.org/10.1080/02626667.2020.1810253.
Hubbard, M., Germida, J., Vujanovic, V., 2012 Feb. Fungal endophytes improve wheat seed germination under heat and drought stress. Botany 90 (2), 137–149. https://doi.org/10.1139/b11-091.
Intergovernmental Panel on Climate Change (IPCC). Mediterranean Region. In: climate Change 2022 – Impacts, Adaptation and Vulnerability: working Group II Contribution to the Sixth Assessment Report of the Intergovernmental Panel on Climate Change. Cambridge: Cambridge University Press; 2022. p. 2233–72. https://doi.org/10.1017/9781009325844.021.
Jagannathan, K.A., 2019. Ready-to-use?-Bridging the Climate Science-Usability Gap For Adaptation. University of California, Berkeley.
Jägermeyr J., Müller C., Ruane A.C., Elliott J., Balkovic J., Castillo O., Faye B., Foster I., Folberth C., Franke J.A., Fuchs K. Climate impacts on global agriculture emerge earlier in new generation of climate and crop models. *Nat. Food*. 2021 Nov;2(11): 873–885. https://doi.org/10.1038/s43016-021-00400-y.
Kaur, G., Singh, G., Motavalli, P.P., Nelson, K.A., Orlowski, J.M., Golden, B.R., 2020 May. Impacts and management strategies for crop production in waterlogged or flooded soils: a review. Agron. J 112 (3), 1475–1501. https://doi.org/10.1002/agj2.20093.
Kelley, M., Schmidt, G.A., Nazarenko, L.S., Bauer, S.E., Ruedy, R., Russell, G.L., Ackerman, A.S., Aleinov, I., Bauer, M., Bleck, R., Canuto, V., Cesana, G., Cheng, Y., Clune, T.L., Cook, B.I., Cruz, C.A., Del Genio, A.D., Elsaesser, G.S., Faluvegi, G., Kiang, N.Y., Kim, D., Lacis, A.A., Leboissetier, A., LeGrande, A.N., Lo, K.K., Marshall, J., Matthews, E.E., McDermid, S., Mezuman, K., Miller, R.L., Murray, L.T., Oinas, V., Orbe, C., García-Pando, C.P., Perlwitz, J.P., Puma, M.J., Rind, D., Romanou, A., Shindell, D.T., Sun, S., Tausnev, N., Tsigaridis, K., Tselioudis, G., Weng, E., Wu, J., Yao, M.-S, 2020 Aug. GISS-E2.1: configurations and climatology. J. Adv. Model. Earth Syst. 12 (8), e2019MS002025 https://doi.org/10.1029/2019MS002025.
Kendall, M.G., 1948. Rank correlation methods. Charles Griffin 160pp.
Konduri V.S., Vandal T.J., Ganguly S., Ganguly A.R. Data science for weather impacts on crop yield. *Front. Sustain. Food Syst*. 2020 May 19; 4:52. https://doi.org/10.3389/fsufs.2020.00052.
Kourat, T., Smadhi, D., Madani, A., 2022 Mar 23. Modeling the impact of future climate change impacts on rainfed durum wheat production in Algeria. Climate 10 (4), 50. https://doi.org/10.3390/cli10040050.
Kumar, L., Chhogyel, N., Gopalakrishnan, T., Hasan, M.K., Jayasinghe, S.L., Kariyawasam, C.S., Kogo, B.K., Ratnayake, S., 2022 Jan 1. Climate change and future of agri-food production. InFuture Foods. Academic Press, pp. 49–79. https://doi.org/10.1016/B978-0-323-91001-9.00009-8.
Lampurlanés J., Plaza-Bonilla D., Álvaro-Fuentes J., Cantero-Martínez C. Long-term analysis of soil water conservation and crop yield under different tillage systems in Mediterranean rainfed conditions. *Field Crops Res.*. 2016 Mar 15; 189:59–67. https://doi.org/10.1016/j.fcr.2016.02.010.
Latiri, K., Lhomme, J.P., Annabi, M., Setter, T.L., 2010 Jul 1. Wheat production in Tunisia: progress, inter-annual variability and relation to rainfall. Europ. J. Agron 33 (1), 33–42. https://doi.org/10.1016/j.eja.2010.02.004.
Lehner, F., Deser, C., Terray, L., 2017 Oct 1. Toward a new estimate of "time of emergence" of anthropogenic warming: insights from dynamical adjustment and a large initial-condition model ensemble. J. Clim 30 (19), 7739–7756. https://doi.org/10.1175/JCLI-D-16-0792.1.
Le Page M., Zribi M. Analysis and predictability of drought in Northwest Africa using optical and microwave satellite remote sensing products. *Sci. Rep*. 2019 Feb 6; 9(1): 1466. https://doi.org/10.1038/s41598-018-37911-x.
Lee, J., Kim, J., Sun, M.A., Kim, B.H., Moon, H., Sung, H.M., Kim, J., Byun, Y.H., 2020 Aug. Evaluation of the Korea meteorological administration advanced community earth-system model (K-ACE). Asia-Pacific J. Atmosph. Sci 56, 381–395. https://doi.org/10.1007/s13143-019-00144-7.
Lesk, C., Anderson, W., Rigden, A., Coast, O., Jägermeyr, J., McDermid, S., Davis, K.F., Konar, M., 2022 Dec. Compound heat and moisture extreme impacts on global crop yields under climate change. Nat. Rev. Earth Environ 3 (12), 872–889. https://doi.org/10.1038/s43017-022-00368-8.
Li, L., Yu, Y., Tang, Y., Lin, P., Xie, J., Song, M., Dong, L., Zhou, T., Liu, L., Wang, L., Pu, Y., Chen, X., Chen, L., Xie, Z., Liu, H., Zhang, L., Huang, X., Feng, T., Zheng, W., Xia, K., Liu, H., Liu, J., Wang, Y., Wang, L., Jia, B., Xie, F., Wang, B., Zhao, S., Yu, Z., Zhao, B., Wei, J., 2020 Sep. The flexible global ocean-atmosphere-land system model grid-point version 3 (FGOALS-g3): description and evaluation. J. Adv. Model. Earth Syst. 12 (9), e2019MS002012 https://doi.org/10.1029/2019MS002012.
Licaj I., Felice D., Germinario C., Zanotti C., Fiorillo A., Marra M., Rocco M. An artificial intelligence-integrated analysis of the effect of drought stress on root traits of

"modern" and "ancient" wheat varieties. Front. Plant Sci. 2023 Oct 13; 14:1241281. https://doi.org/10.3389/fpls.2023.1241281.
Liu B., Liu L., Tian L., Cao W., Zhu Y., Asseng S. Post-heading heat stress and yield impact in winter wheat of China. Global Change Biol.. 2014 Feb; 20(2):372–381. https://doi.org/10.1111/gcb.12442.
Liu L., Zhang X. Effects of temperature variability and extremes on spring phenology across the contiguous United States from 1982 to 2016. Scientif. Reports. 2020 Oct 21; 10(1):17952. https://doi.org/10.1038/s41598-020-74804-4.
Lizaso, J.I., Ruiz-Ramos, M., Rodríguez, L., Gabaldon-Leal, C., Oliveira, J.A., Lorite, I.J., Sánchez, D., García, E., Rodríguez, A., 2018 Feb 1. Impact of high temperatures in maize: phenology and yield components. Field Crops Res. 216, 129–140. https://doi.org/10.1016/j.fcr.2017.11.013.
Lovato, T., Peano, D., Butenschön, M., Materia, S., Iovino, D., Scoccimarro, E., Fogli, P. G., Cherchi, A., Bellucci, A., Gualdi, S., Masina, S., 2022 Mar. CMIP6 simulations with the CMCC Earth system model (CMCC-ESM2). J.Adv. Model. Earth Syst 14 (3), e2021MS002814. https://doi.org/10.1029/2021MS002814.
Mahrookashani, A., Siebert, S., Hüging, H., Ewert, F., 2017 Dec. Independent and combined effects of high temperature and drought stress around anthesis on wheat. J. Agron. Crop Sci. 203 (6), 453–463. https://doi.org/10.1111/jac.12218.
Mann, H.B., 1945 Jul 1. Nonparametric tests against trend. Econometrica. J. Econom. Soc 245–259.
Maraun, D., Widmann, M., 2018 Jan 18. Statistical Downscaling and Bias Correction For Climate Research. Cambridge University Press. https://doi.org/10.1017/9781107588783.
Masson D., Knutti R. Climate model genealogy. *Geophys. Res. Lett.* 2011 Apr 28;38(8). https://doi.org/10.1029/2011GL046864.
Mirgol, B., Dieppois, B., Northey, J., Eden, J., Jarlan, L., Tramblay, Y., Mahé, G., El Hazdour, I., Khabba, S., Hanich, L., Le Page, M, 2023 May. Recent trends in vegetation phenology across the southern Mediterranean region, and potential climatic drivers. InEGU General Assem. Conference Abstracts EGU-15331. https://doi.org/10.5194/egusphere-egu23-15331.
Mirgol, B., Dieppois, B., Northey, J., Eden, J., Jarlan, L., Khabba, S., Le Page, M., Mahé, G, 2024 Mar 7. Emerging extreme climate-related stresses over croplands and wheat-harvested areas in the southern Mediterranean region during the 21st century. Copernicus Meetings. https://doi.org/10.5194/egusphere-egu24-13371.
Mirgol B., Nazari M., Eteghadipour M. Modelling climate change impact on irrigation water requirement and yield of winter wheat (Triticum aestivum L.), barley (Hordeum vulgare L.), and fodder maize (Zea mays L.) in the semi-arid Qazvin Plateau, Iran. *Agriculture*. 2020 Mar 3;10(3):60. https://doi.org/10.3390/agriculture10030060.
Muñoz-Sabater, J., Dutra, E., Agustí-Panareda, A., Albergel, C., Arduini, G., Balsamo, G., Boussetta, S., Choulga, M., Harrigan, S., Hersbach, H., Martens, B., Miralles, D.G., Piles, M., Rodríguez-Fernández, N.J., Zsoter, E., Buontempo, C., Thépaut, J-N, 2021 Sep 7. ERA5-Land: A state-of-the-art global reanalysis dataset for land applications. Earth Syst. Sci. Data 13 (9), 4349–4383. https://doi.org/10.5194/essd-13-4349-2021.
Nazari M., Mirgol B., Salehi H. Climate change impact assessment and adaptation strategies for rainfed wheat in contrasting climatic regions of Iran. *Front. Agron.*. 2021 Dec 20; 3:806146. https://doi.org/10.3389/fagro.2021.806146.
Nin-Pratt A., El-Enbaby H., Figueroa J.L., ElDidi H., Breisinger C. Agriculture and economic transformation in the Middle East and North Africa: a review of the past with lessons for the future. 2017. https://doi.org/10.2499/9780896292956.
Noto L.V., Cipolla G., Pumo D., Francipane A. Climate change in the Mediterranean Basin (Part II): a review of challenges and uncertainties in climate change modeling and impact analyses. *Water Resour. Manag.* 2023 May; 37(6):2307–2323. https://doi.org/10.1007/s11269-023-03444-w.
O'Neill, B.C., Carter, T.R., Ebi, K., Harrison, P.A., Kemp-Benedict, E., Kok, K., Kriegler, E., Preston, B.L., Riahi, K., Sillmann, J., van Ruijven, B.J., van Vuuren, D., Carlisle, D., Conde, C., Fuglestvedt, J., Green, C., Hasegawa, T., Leininger, J., Monteith, S., 2020 Dec. Pichs-Madruga R. Achievements and needs for the climate change scenario framework. Nat. Clim. Chang 10 (12), 1074–1084. https://doi.org/10.1038/s41558-020-00952-0.
Ostberg, S., Schewe, J., Childers, K., Frieler, K., 2018 May 9. Changes in crop yields and their variability at different levels of global warming. Earth Syst. Dynamics 9 (2), 479–496. https://doi.org/10.5194/esd-9-479-2018.
Parker, L., Pathak, T., Ostoja, S., 2021 Mar 25. Climate change reduces frost exposure for high-value California orchard crops. Sci. Total Environ 762, 143971. https://doi.org/10.1016/j.scitotenv.2020.143971.
Portmann F.T., Siebert S., Döll P. MIRCA2000—Global monthly irrigated and rainfed crop areas around the year 2000: a new high-resolution data set for agricultural and hydrological modeling. *Global Biogeochem. Cycles*. 2010 Mar; 24(1). https://doi.org/10.1029/2008GB003435.
Rashid M.A., Andersen M.N., Wollenweber B., Kørup K., Zhang X., Olesen J.E. Impact of heat-wave at high and low VPD on photosynthetic components of wheat and their recovery. *Environ. Exp. Bot.*. 2018 Mar 1; 147:138–146. https://doi.org/10.1016/j.envexpbot.2017.12.009.
Ray D.K., Gerber J.S., MacDonald G.K., West P.C. Climate variation explains a third of global crop yield variability. *Nat. Commun.* 2015 Jan 22; 6(1):5989. https://doi.org/10.1038/ncomms6989.
Raymond, F., Ullmann, A., Tramblay, Y., Drobinski, P., Camberlin, P., 2019 Dec. Evolution of Mediterranean extreme dry spells during the wet season under climate change. Reg. Environ. Change 19, 2339–2351. https://doi.org/10.1007/s10113-019-01526-3.
Ribeiro, A.F., Russo, A., Gouveia, C.M., Páscoa, P., Zscheischler, J., 2020 Oct 9. Risk of crop failure due to compound dry and hot extremes estimated with nested copulas. Biogeosciences 17 (19), 4815–4830. https://doi.org/10.5194/bg-17-4815-2020.
Saadi, S., Todorovic, M., Tanasijevic, L., Pereira, L.S., Pizzigalli, C., Lionello, P., 2015 Jan 1. Climate change and Mediterranean agriculture: impacts on winter wheat and tomato crop evapotranspiration, irrigation requirements and yield. Agric. Water Manag. 147, 103–115. https://doi.org/10.1016/j.agwat.2014.05.008.
Schilling, J., Freier, K.P., Hertig, E., Scheffran, J., 2012 Aug 1. Climate change, vulnerability and adaptation in North Africa with focus on Morocco. Agric. Ecosyst. Environ 156, 12–26. https://doi.org/10.1016/j.agee.2012.04.021.
Schilling, J., Hertig, E., Tramblay, Y., Scheffran, J., 2020 Mar. Climate change vulnerability, water resources and social implications in North Africa. Reg. Environ. Change 20, 1–12. https://doi.org/10.1007/s10113-020-01597-7.
Séférian, R., Nabat, P., Michou, M., Saint-Martin, D., Voldoire, A., Colin, J., Decharme, B., Delire, C., Berthet, S., Chevallier, M., Sénési, S., Franchisteguy, L., Vial, J., Mallet, M., Joetzjer, E., Geoffroy, O., Guérémy, J.-F., Moine, M.-P., Msadek, R., Ribes, A., Rocher, M., Roehrig, R., Salas-y-Mélia, D., Sanchez, E., Terray, L., Valcke, S., Waldman, R., Aumont, O., Bopp, L., Deshayes, J., Éthé, C., Madec, G., 2019. Evaluation of CNRM Earth system model, CNRM-ESM2-1: role of Earth system processes in present-day and future climate. J. Adv. Model. Earth Syst. 11 (12), 4182–4227. https://doi.org/10.1029/2019MS001791, 2019 Dec.
Seland Ø., Bentsen M., Olivié D., Toniazzo T., Gjermundsen A., Graff L.S., Debernard J.B., Gupta A.K., He Y.C., Kirkevåg A., Schwinger J. Overview of the norwegian earth system model (NorESM2) and key climate response of CMIP6 DECK, historical, and scenario simulations. Geoscientif. Model Develop. 2020 Dec 4;13(12):6165–6200. https://doi.org/10.5194/gmd-13-6165-2020.
Seleiman, M.F., Al-Suhaibani, N., Ali, N., Akmal, M., Alotaibi, M., Refay, Y., Dindaroglu, T., Abdul-Wajid, H.H., Battaglia, M.L., 2021. Drought stress impacts on plants and different approaches to alleviate its adverse effects. Plants 10 (2), 259. https://doi.org/10.3390/plants10020259.
Sellar, A.A., Jones, C.G., Mulcahy, J.P., Tang, Y., Yool, A., Wiltshire, A., O'Connor, F.M., Stringer, M., Hill, R., Palmieri, J., Woodward, S., de Mora, L., Kuhlbrodt, T., Rumbold, S.T., Kelley, D.I., Ellis, R., Johnson, C.E., Walton, J., Abraham, N.L., Andrews, M.B., Andrews, T., Archibald, A.T., Berthou, S., Burke, E., Blockley, E., Carslaw, K., Dalvi, M., Edwards, J., Folberth, G.A., Gedney, N., Griffiths, P.T., Harper, A.B., Hendry, M.A., Hewitt, A.J., Johnson, B., Jones, A., Jones, C.D., Keeble, J., Liddicoat, S., Morgenstern, O., Parker, R.J., Predoi, V., Robertson, E., Siahaan, A., Smith, R.S., Swaminathan, R., Woodhouse, M.T., Zeng, G., Zerroukat, M, 2019 Dec. UKESM1: description and evaluation of the UK Earth System Model. J. Adv. Model. Earth Syst 11 (12), 4513–4558. https://doi.org/10.1029/2019MS001739.
Singh, B.K., Delgado-Baquerizo, M., Egidi, E., Guirado, E., Leach, J.E., Liu, H., Trivedi, P., 2023 Oct. Climate change impacts on plant pathogens, food security and paths forward. Nat. Rev. Microbiol 21 (10), 640–656. https://doi.org/10.1038/s41579-023-00900-7.
Skendžić S., Zovko M., Živković I.P., Lešić V., Lemić D. The impact of climate change on agricultural insect pests. Insects. 2021 May 12; 12(5):440. https://doi.org/10.3390/insects12050440.
Spagnuolo F., W.Cramer, Ali P. 2022. *Mediterranean region in: climate Change 2022: impacts, adaptation, and vulnerability. contribution of WG II to the 6AR of the intergovernmental panel on climate change*. 2022. pp.2233–2272. DOI: https://doi.org/10.1017/9781009325844.021.
Statista Search Department, 2024, May 2nd. Export value of leading agri-food items from Morocco as of 2022, by type [Infographic]. Statista. https://www.statista.com/statistics/1234232/export-value-of-leading-agri-foods-and-seafoods-in-morocco/.
Statista Search Department, 2024b. Export value of agricultural products from Algeria in 2020, by product [Infographic]. Statista. https://www.statista.com/statistics/1303002/export-value-of-agricultural-products-from-algeria-by-product/.
Statista Search Department, 2024, May 2nd. Export of the leading food and agricultural products from Tunisia from 2020 to 2021[Infographic]. Statista. https://www.statista.com/statistics/1289729/export-of-leading-food-products-from-tunisia/.
Suresh, Munjal R. Adaptation and tolerance of wheat to heat stress. *Plant Ecophysiol. Adapt. Climate Change*. 2020:331–42. https://doi.org/10.1007/978-981-15-2156-0_11.
Swart N.C., Cole J.N., Kharin V.V., Lazare M., Scinocca J.F., Gillett N.P., Anstey J., Arora V., Christian J.R., Hanna S., Jiao Y., Swart N.C., Cole J.N.S., Kharin V.V., Lazare M., Scinocca J.F., Gillett N.P., Anstey J., Arora V., Christian J.R., Hanna S., Jiao Y., Lee W.G., Majaess F., Saenko O.A., Seiler C., Seinen C., Shao A., Sigmond M., Solheim L., von Salzen K., Yang D., Winter B.The Canadian earth system model version 5 (CanESM5. 0.3). *Geoscientif. Model Develop*. 2019 Nov 25;12(11):4823–4873. https://doi.org/10.5194/gmd-12-4823-2019.
Takemura T. MIROC MIROC6 model output prepared for CMIP6 AerChemMIP. *Earth Syst. Grid Feder*. 2019. https://doi.org/10.22033/ESGF/CMIP6.9121.
Tang, W., Cui, L., Zheng, S., Hu, W., 2022 Sep 28. Multi-scenario simulation of land use carbon emissions from energy consumption in Shenzhen. China. *Land* 11 (10), 1673. https://doi.org/10.3390/land11101673.
Tarín-Carrasco, P., Petrova, D., Chica-Castells, L., Lukovic, J., Rodó, X., Cvijanovic, I., 2024 Jan 5. Assessment of future precipitation changes in mediterranean climate regions from CMIP6 ensemble. EGUsphere 2024, 1–34. https://doi.org/10.5194/egusphere-2023-3057.
Thrasher B., Maurer E.P., McKellar C., Duffy P.B. Bias correcting climate model simulated daily temperature extremes with quantile mapping. *Hydrol. Earth Syst. Sci.*. 2012 Sep 17;16(9):3309–3314. https://doi.org/10.5194/hess-16-3309-2012.
Thrasher B., Wang W., Michaelis A., Melton F., Lee T., Nemani R. NASA global daily downscaled projections, CMIP6. *Sci. Data*. 2022 Jun 2; 9(1):262. https://doi.org/10.1038/s41597-022-01393-4.
Tramblay, Y., Koutroulis, A., Samaniego, L., Vicente-Serrano, S.M., Volaire, F., Boone, A., Le Page, M., Llasat, M.C., Albergel, C., Burak, S., Cailleret, M, 2020 Nov 1. Challenges for drought assessment in the Mediterranean region under future climate

scenarios. Earth-Sci. Rev. 210, 103348 https://doi.org/10.1016/j.earscirev.2020.103348.
Urdiales-Flores D., Zittis G., Hadjinicolaou P., Osipov S., Klingmüller K., Mihalopoulos N., Kanakidou M., Economou T., Lelieveld J. Drivers of accelerated warming in Mediterranean climate-type regions. *npj Climate and Atmospheric Science*. 2023 July 20;6(1):97. https://doi.org/10.1038/s41612-023-00423-1.
U.S. Department of Agriculture (USDA) Foreign Agricultural Service, 2024, May 22nd. Crop Explorer - World Agricultural Production (WAP) Briefs - North Africa. https://ipad.fas.usda.gov/cropexplorer/pecad_stories.aspx?regionid=na&ftype=prodbriefs.
Van Dijk, M., Morley, T., Rau, M.L., Saghai, Y., 2021 Jul. A meta-analysis of projected global food demand and population at risk of hunger for the period 2010–2050. Nature Food 2 (7), 494–501. https://doi.org/10.1038/s43016-021-00322-9.
Velásquez, A.C., Castroverde, C.D., He, S.Y., 2018 May 21. Plant–pathogen warfare under changing climate conditions. Curr. Biol 28 (10), R619–R634. https://doi.org/10.1016/j.cub.2018.03.054.
Velpuri M., Das J., Umamahesh N.V. Spatio-temporal compounding of connected extreme events: projection and hotspot identification. *Environ. Res.*. 2023 Oct 15; 235:116615. https://doi.org/10.1016/j.envres.2023.116615.
Vicente-Serrano, S.M., Beguería, S., López-Moreno, J.I., 2010 Apr 1. A multiscalar drought index sensitive to global warming: the standardized precipitation evapotranspiration index. J. Clim 23 (7), 1696–1718. https://doi.org/10.1175/2009JCLI2909.1.
Vogel J., Paton E., Aich V., Bronstert A. Increasing compound warm spells and droughts in the Mediterranean Basin. *Weather Climate Extr*. 2021 June 1; 32:100312. https://doi.org/10.1016/j.wace.2021.100312.
Volodin E., Mortikov E., Gritsun A., Lykossov V., Galin V., Diansky N., Gusev A., Kostrykin S., Iakovlev N., Shestakova A., Emelina S. INM INM-CM5-0 model output prepared for CMIP6 CMIP amip. Earth Syst. Grid Feder. 2019. https://doi.org/10.22033/ESGF/CMIP6.5081.
Wang F., Shao W., Yu H., Kan G., He X., Zhang D., Ren M., Wang G. *Re*-evaluation of the power of the Mann-Kendall test for detecting monotonic trends in hydrometeorological time series. *Front. Earth Sci*. 2020 Feb 6; 8:14. https://doi.org/10.3389/feart.2020.00014.
Wieners K.-.H., Giorgetta M., Jungclaus J., Reick C., Esch M., Bittner M., Legutke S., Schupfner M., Wachsmann F., Gayler V., Haak H., de Vrese P., Raddatz T., Mauritsen T., von Storch J.-.S., Behrens J., Brovkin V., Claussen M., Crueger T., Fast I., Fiedler S., Hagemann S., Hohenegger C., Jahns T., Kloster S., Kinne S., Lasslop G., Kornblueh L., Marotzke J., Matei D., Meraner K., Mikolajewicz U., Modali K., Müller W., Nabel J., Notz D., Peters-von Gehlen K., Pincus R., Pohlmann H., Pongratz J., Rast S., Schmidt H., Schnur R., Schulzweida U., Six K., Stevens B., Voigt A., Roeckner E. MPI-M MPI-ESM1.2-LR model output prepared for CMIP6 CMIP historical. *Earth Syst. Grid Feder*. 2019. https://doi.org/10.22033/ESGF/CMIP6.4403.
Wilcoxon, F., 1945. Individual comparisons by ranking methods. Biomet. Bull. 1 (6), 80–83. https://doi.org/10.2307/3001968.
Wood A.W., Leung L.R., Sridhar V., Lettenmaier D.P. Hydrologic implications of dynamical and statistical approaches to downscaling climate model outputs. *Climatic Change*. 2004 Jan; 62:189–216. https://doi.org/10.1023/B:CLIM.0000013685.99609.9e.
Wu T., Zhang F., Zhang J., Jie W., Zhang Y., Wu F., Li L., Yan J., Liu X., Lu X., Tan H. Beijing Climate Center Earth System Model version 1 (BCC-ESM1): model description and evaluation of aerosol simulations. *Geoscientif. Model Develop*. 2020 Mar 6; 13(3):977–1005. https://doi.org/10.5194/gmd-13-977-2020.
Yang C., Fraga H., van Ieperen W., Santos J.A. Assessing the impacts of recent-past climatic constraints on potential wheat yield and adaptation options under Mediterranean climate in southern Portugal. *Agric. Syst*. 2020 June 1; 182:102844. https://doi.org/10.1016/j.agsy.2020.102844.
Yu, H., Zhang, Q., Sun, P., Song, C., 2018 Sep. Impact of droughts on winter wheat yield in different growth stages during 2001–2016 in Eastern China. Int. J. Disaster Risk Sci 9, 376–391. https://doi.org/10.1007/s13753-018-0187-4.
Yue, S., Pilon, P., Cavadias, G., 2002 Mar 1. Power of the Mann–Kendall and Spearman's rho tests for detecting monotonic trends in hydrological series. J. Hydrol 259 (1–4), 254–271. https://doi.org/10.1016/S0022-1694(01)00594-7.
Yukimoto S., Koshiro T., Kawai H., Oshima N., Yoshida K., Urakawa S., Tsujino H., Deushi M., Tanaka T., Hosaka M., Yoshimura H., Shindo E., Mizuta R., Ishii M., Obata A., Adachi Y. *MRI MRI-ESM2.0 model output prepared for CMIP6 CMIP. World Data Center for Climate (WDCC) at DKRZ*. 2019. https://www.wdc-climate.de/ui/entry?acronym=C6_5243961.
Zalidis G., Stamatiadis S., Takavakoglou V., Eskridge K., Misopolinos N. Impacts of agricultural practices on soil and water quality in the Mediterranean region and proposed assessment methodology. *Agric. Ecosyst. Environ*. 2002 Feb 1; 88(2): 137–146. https://doi.org/10.1016/S0167-8809(01)00249-3.
Zampieri M., Ceglar A., Dentener F., Toreti A. Wheat yield loss attributable to heat waves, drought and water excess at the global, national and subnational scales. *Environ. Res. Lett*. 2017 June 5; 12(6):064008. https://doi.org/10.1088/1748-9326/aa723b.
Zampieri M., Toreti A., Ceglar A., Naumann G., Turco M., Tebaldi C. Climate resilience of the top ten wheat producers in the Mediterranean and the Middle East. Regional Environmental Change. 2020 Jun; 20:1–9. https://doi.org/10.1007/s10113-020-01622-9.
Zhang, L., Chu, Q.Q., Jiang, Y.L., Fu, C.H., Lei, Y.D., 2021 Oct 1. Impacts of climate change on drought risk of winter wheat in the North China Plain. J. Integr. Agric 20 (10), 2601–2612. https://doi.org/10.1016/S2095-3119(20)63273-7.
Zhu, T., Fonseca De Lima, C.F., De Smet, I., 2021 Nov 20. The heat is on: how crop growth, development, and yield respond to high temperature. J. Exp. Bot. 72 (21), 7359–7373.
Zittis G., Bruggeman A., Lelieveld J. Revisiting future extreme precipitation trends in the Mediterranean. *Weather Climate Extremes*. 2021 Dec 1; 34:100380. https://doi.org/10.1016/j.wace.2021.100380.
Zribi, M., Brocca, L., Molle, F., Tramblay, Y., 2020. Introduction. In: Zribi, M, Brocca, L, Tramblay, Y, Molle, F (Eds.), Water Resources in the Mediterranean Region. https://doi.org/10.1016/B978-0-12-818086-0.09990-8 xv–xix.
Zscheischler J., Martius O., Westra S., Bevacqua E., Raymond C., Horton R.M., van den Hurk B., AghaKouchak A., Jézéquel A., Mahecha M.D., Maraun D. A typology of compound weather and climate events. *Nat. Rev. Earth & Environ*. 2020 Jul; 1(7): 333–347. https://doi.org/10.1038/s43017-020-0060-z.